DEPARTMENT OF THE NAVY

DAVID TAYLOR MODEL BASIN
WASHINGTON, D.C.

[redacted]

HYDROMECHANICS

O

AERODYNAMICS

O

STRUCTURAL MECHANICS

O

APPLIED MATHEMATICS

O

ACOUSTICS AND VIBRATION

MOBILITY AND SOUND RADIATION MEASUREMENTS ON A CYLINDRICAL GLASS-REINFORCED-PLASTIC MODEL

by

Dwight L. Ludwig and
Christopher J. Noonan

ACOUSTICS AND VIBRATION LABORATORY

RESEARCH AND DEVELOPMENT REPORT

November 1964

Report 1867

PRNC-TMB-648 (Rev 1-64)

DEPARTMENT OF THE NAVY
DAVID TAYLOR MODEL BASIN
WASHINGTON, D.C. - 20007

IN REPLY REFER TO
9870.1
3900/Noise
5605
964:CJN:ec
14 December 1964

From: Commanding Officer and Director, David Taylor Model Basin
To: Chief, Bureau of Ships (345) (in duplicate)

Subj: David Taylor Model Basin Report 1867; transmittal of

Ref: (a) BUSHIPS ltr F013 0503 Ser 634 C3-438 of 9 May 1962

Encl: (1) DTMB Report 1867, "Mobility and Sound Radiation Measurements on a Cylindrical Glass-Reinforced-Plastic Model" November 1964

1. By reference (a) the Bureau of Ships authorized the David Taylor Model Basin to measure the vibratory and sound radiation characteristics of glass-reinforced plastic models.

2. Enclosure (1) contains data on drive-point mobility, an estimate of damping ratio, mode shapes of resonant frequencies, radiated sound pressure level versus frequency, and sound pressure directivity patterns at resonant frequencies in the frequency range 200 to 5300 cps for an internally ring stiffened cylindrical model having 6" ID and 28" length.

E. F. Noonan

E. F. Noonan
By direction

9870.1
3900/Noise
5605
964:CJN:ec
14 December 1964

Copy to:
BUSHIPS (634C), with 9 copies of encl (1)
(320), with 1 copy of encl (1)
(210L), with 3 copies of encl (1)
(341A), with 1 copy of encl (1)
(342A), with 1 copy of encl (1)
(420), with 1 copy of encl (1)
(421), with 1 copy of encl (1)
(423), with 1 copy of encl (1)
(440), with 1 copy of encl (1)
(442), with 1 copy of encl (1)
(443), with 1 copy of encl (1)
(525), with 2 copies of encl (1)
(633), with 1 copy of encl (1)
(651F), with 1 copy of encl (1)
BUDOCKS, Attn: C-423, with 1 copy of encl (1)
CHONR (104), with 1 copy of encl (1)
(419), with 1 copy of encl (1)
(439), with 1 copy of encl (1)
(466), with 1 copy of encl (1)
CNO (OP 07T), with 1 copy of encl (1)
(OP 311), with 1 copy of encl (1)
(OP 713), with 1 copy of encl (1)
(OP 725), with 1 copy of encl (1)
CO U.S. Naval Applied Sci Lab (9350), with 2 copies of encl (1)
BUWEPS (RRMA), with 1 copy of encl (1)
(RMMP-23), with 1 copy of encl (1)
Special Projects Office
S6-27012 (Mr. H. Bernstein), with 1 copy of encl (1)
CDR, USNOL (W Dept), with 1 copy of encl (1)
(WM Div), with 1 copy of encl (1)
DIR, USNRL (2027), with 1 copy of encl (1)
(6120), with 1 copy of encl (1)
(6210), with 1 copy of encl (1)
DIR, Plastics Tech Evaluation Center, Picatinny Arsenal, Dover, with 2 copies of encl (1)

9870.1
3900/Noise
5605
964:CJN:ec
14 December 1964

Copy to: (continued)
CDR, USNOTS (5557), China Lake, with 1 copy of encl (1)
US NAVAL ORDNANCE TEST STATION, (Mr. J.L. Phillips P-8082)
Pasadena, California, with 1 copy of encl (1)
CDR, DDC, with 20 copies of encl (1)
CO & DIR, USMEL, with 1 copy of encl (1)
CO & DIR, USNUSL, with 1 copy of encl (1)
CO & DIR, USNEL, with 1 copy of encl (1)
CO USNROTC & NAVADMIN U, MIT, with 1 copy of encl (1)
CO, USNUOS, with 1 copy of encl (1)
CIR of Def R & E, Attn: Tech Lib, with 1 copy of encl (1)
NAVSHIPYD PTSMH, with 2 copies of encl (1)
O-in-C, PGSCOL, Webb Inst, with 1 copy of encl (1)
Dir, APL, Univ of Wash, Seattle, with 1 copy of encl (1)
NAS, Attn: Comm on Undersea Warfare, with 1 copy of encl (1)
CO & DIR, USMDL, with 1 copy of encl (1)
Commanding General
Aeronautical Systems Div, with 2 copies of encl (1)
(ASRCNC-1) Wright Patterson
Air Force Base, Ohio
Aerojet-General Corp., (Mr. S. Stokes) Azusa, Calif., with 1 copy of encl (1)
NARMCO Research & Dev Div of Telecomputing Corp.,
San Diego, Calif.
(Mr. B. Duft), with 1 copy of encl (1)
Armour Research Foundation
(Dr. J. W. Dally)
Illinois Inst of Tech
Chicago, Ill., with 1 copy of encl (1)
(Gen Motors Corp.) (Dr. R.B. Costello) Def Systems Div.,
Santa Barbara Lab
Santa Barbara, Calif., with 1 copy of encl (1)
Battelle Memorial Inst (Dr. R. Leininger) Columbus, Ohio, with 1 copy of encl (1)
H. I. Thompson Fiberglass (Mr. N. Meyers), Gardena, Calif., with 1 copy
of encl (1)
Owens-Corning Fiberglass Corp. (Mr. R.J. Weaver), Washington, D.C.
with 1 copy of encl (1)
U. S. Rubber Research Center (Mr. F. Francois, Jr.), Wayne, N. J.,
with 1 copy of encl (1)
Shell Chemical Co. (Mr. R. E. Bayes), Plastics & Resin Div., N. Y., N. Y.
with 1 copy of encl (1)

9870.1
3900/Noise
5605
964:CJN:ec
14 December 1964

Copy to: (continued)
North American Aviation Inc. (Mr. R. Gorcey)
Rocketdyne Div
Canoga Park, Calif., with 1 copy of encl (1)
Hercules Powder Co. (Mr. J.A. Scherer) Wilmington, Del., with 1 copy of encl (1)
Brunswick Corp. (Mr. W. McKay), Marion, Va., with 1 copy of encl (1)
Douglas Aircraft Corp. (Mr. J.H. Cunningham),
Missile & Space Systems Div.
Santa Monica, Calif., with 1 copy of encl (1)
Goodyear Aircraft Corp.
1210 Massillon Rd.
Akron, Ohio, with 1 copy of encl (1)
A. O. Smith Corporation, Milwaukee, Wisconsin
(Mr. W. A. Deringer), with 1 copy of encl (1)
University of Ill.
(Prof H. R. Corten)
Dept of T & M
Urbana, Ill., with 1 copy of encl (1)
AVCO Corp.
Undersea Projects Directorate, Wilmington, Mass., with 1 copy of encl (1)
Union Carbide Plastics Corp.,
(Mr. Charles Platt)
Brunswick, N. J., with 1 copy of encl (1)

MOBILITY AND SOUND RADIATION MEASUREMENTS ON A CYLINDRICAL GLASS-REINFORCED-PLASTIC MODEL

by

Dwight L. Ludwig and
Christopher J. Noonan

November 1964

Report 1867
S-F013 05 03

TABLE OF CONTENTS

LIST OF FIGURES

LIST OF TABLES

ABSTRACT

Vibration and sound radiation characteristics are determined for a 6-in. ID, 28-in. long, internally ring-stiffened, glass-reinforced-plastic cylinder in the frequency range of 200 to 5300 cps. Drive-point mobility, an estimate of damping ratio, the mode shapes of resonant frequencies, the radiated sound pressure levels versus frequency, and the sound pressure directivity patterns at resonances are presented.

INTRODUCTION

Glass-reinforced-plastic laminates have been in service for about 10 years. They have been used for fairwater structure, radar domes, sonar domes, etc. The David Taylor Model Basin has pressure-tested several glass-reinforced-plastic cylinders which indicate that considerable weight saving in hull structure can be realized and appear to have great promise as a structure for deep-diving submersibles.

The David Taylor Model Basin was authorized to measure the vibratory characteristics of glass-reinforced-plastic cylindrical models.[1] The mobility method was used to obtain data comparable with existing methods of evaluation.

Preliminary work with Model RV-8 (Figure 1) began in December 1962. Tests in water performed in the summer of 1963 at the NOL Brighton Dam Facility are reported herein. Originally planned air tests were not run.

CYLINDRICAL TEST MODEL

Details of the glass-reinforced-plastic test model, RV-8, are shown in Figure 1. Photographs of the model with the end plates and the instrumentation housing are shown in Figure 2. The end plates are 9 in. in diameter, are 2 1/2 in. thick, weigh approximately 40 lb each and provide negative buoyance.

---

[1] References are listed on page 36.

INSTRUMENTATION AND TEST SITE

A block diagram of the instrumentation used to measure mechanical mobility is shown in Figure 3. The system characteristics are:

Frequency Range - 200 to 5300 cps
Dynamic Range - 40 db
Confidence Limits - 1 db
Writing Speed - 20 in/sec
Paper Speed - 2.5 to 75 in/hr
Time for full-scale vertical deflection - 0.2 sec

The system measures either head acceleration A_H or transfer acceleration A_i ($i = 1$ to 18) over the frequency range while driving the model with a constant force. The force is held constant by a force feedback system and the mobility is directly proportional to a constant times the acceleration divided by the frequency. Figure 4 presents photographs of this measuring system.

The oscillator is swept through its frequency range by a mechanical coupling connected to the drive of the recorder. The oscillator frequency is thereby synchronized with the printed frequency lines on the acceleration and phase records. The phase recorder is electrically connected to the system and simultaneously records the phase angle between any two accelerations measured or between acceleration and applied force.

The model is excited with a TMB miniature impedance head (Serial No. 56). Gages in the impedance head measure the applied force F_H and the drive-point acceleration A_H. Transfer acceleration A_i is measured at 18 locations around and along the model. All gages measured acceleration normal to the surface. The measuring locations are shown in Figure 5 and Figure 6 shows photographs of the physical arrangement. Impedance head characteristics are given in Reference 2.

Sound pressure measurements were made at the Naval Ordnance Laboratory (NOL) Acoustic Facility at Brighton, Maryland. A photograph and layout sketch of the facility is shown in Figure 7. The instrument room of the barge contains the signal source, the heterodyne system, the voltage amplifiers, the pulse equipment, and the strip and polar chart recorders. These are called the low-level racks. All power amplifiers and power

supplies are contained in four similar relay racks, called the high-level racks, located at a 10-ft distance from the low-level racks. The low-level and high-level racks are shown in Figure 8. A block diagram of the electronic equipment used to measure the sound pressure level is shown in Figure 9. This equipment may be divided into three basic components: the continuous wave system, the heterodyne system, and the pulse system.

In the test the continuous wave and the heterodyne systems were used. The continuous wave system was used when the background noise and extraneous signals were insignificant in comparison to the desired signal. The transmitting part of the system consists of an oscillator and a power amplifier, which feeds the signal to the impedance head. The receiving part consists of a hydrophone connected to the low-level amplifier, the driver amplifier, a filter, the recorder amplifier, and either a polar or strip recorder. The calibration amplifier may be substituted for the hydrophone to supply a standard voltage for calibrating the receiving sections over the desired frequency range. The heterodyne system is the same as the continuous wave system except for the insertion of heterodyne circuits. The purpose of this system is to increase the signal-to-noise ratio and to permit most of the amplification and recording to be done at a single frequency. The carrier frequency is 97 kc. The decrease in noise level is accomplished by the use of crystal filters in the receiving circuits. These filters have 10-, 200-, or 3000-cps bandwidth with a center frequency of 97 kc. Frequencies outside these bands are attenuated approximately 40 db. Further information about the test facility is contained in Reference 3.

The sound pressure was measured with a standard hydrophone at a distance of 2 meters from the geometric center of the model. Approximately 25 ft of water was above and below the model. Ambient background noise level for 10 cps passband during tests was approximately 68 db re 0.0002 μ bar for all frequencies except for the 200- to 310-cps range where it was 84 db re 0.0002 μ bar.

Figure 10 shows photographs of the model suspension system. A rotation mechanism is capable of rotating the model 360° while mounted either vertically (longitudinal centerline vertical) or horizontally (longitudinal centerline horizontal).

TEST PROCEDURE

MODEL VERTICAL (longitudinal centerline oriented vertically)

1. Sweep frequency from 200 to 5300 cps and record A_H and $\phi_{A_H F_H}$ with applied force held constant to obtain mobility versus frequency.

2. Sweep frequency from 200 to 5300 cps and record sound pressure levels, with applied voltage held constant to obtain sound pressure level versus frequency.

3. Obtain mode shapes by plotting A_i both circumferential and longitudinal at resonant frequencies ($\phi_{A_H F_H} = 90$ deg) and at frequencies of maximum acceleration A_H max.

4. Obtain directivity patterns around the mid-circumferential plane at frequencies of maximum sound pressure level.

MODEL HORIZONTAL (longitudinal centerline oriented horizontally)

1. Sweep frequency from 200 to 5300 cps and record A_H and $\phi_{A_H F_H}$ with applied force held constant to obtain mobility versus frequency.

2. Sweep frequency from 200 to 5300 cps and record sound pressure levels, with applied voltage held constant to obtain sound pressure level versus frequency.

3. Obtain mode shapes by plotting A_i both circumferential and longitudinal at resonant frequencies ($\phi_{A_H F_H} = 90$ deg) and at frequencies of maximum acceleration A_H max.

4. Obtain directivity patterns around the model in the plane of the longitudinal $\mathbb{Q}_L$ at frequencies of maximum sound pressure level.

TEST RESULTS

Mobility versus frequency for vertical and horizontal orientations are shown in Figure 11. The mobility was derived from the continuous acceleration A_H and phase angle $\phi_{A_H F_H}$ records of which Figure 12 is an example.

Sound pressure versus frequency for the vertical and horizontal orientations is shown in Figure 13.

To determine the mode shapes at resonant frequencies, both phase angle $\phi_{A_H A_i}$ and transfer acceleration A_i were read for these frequencies up to 5300 cps. The data are plotted in Figure 14. All resonant mode shapes

have been plotted as percentages of the maximum measured acceleration for the individual mode because of the wide variation in acceleration for the different resonances. The relative amplitude in these figures is the acceleration, which is in quadrature with the force, multiplied by the cosine of the associated phase angle. The phase angle $\phi_{A_H A_i}$ is expected to vary smoothly along and around the model and, therefore, has been plotted as a monotonic function. All accelerometers were measuring normal to the shell surface. The plot of in-phase components for accelerometers 1 to 10 describes the acceleration distribution "n" (defined as the number of full waves around the mid-circumferential) normal to the surface at the mid-circumferential, (ψ = 0 to 180 deg). The same method applies to the longitudinal axis accelerations, where "m" (defined as the number of half waves along the length of the model) is plotted.

Table 1 is a summary of the resonant frequencies and their associated modal numbers up to 5300 cps as determined from the acceleration distributions in Figure 14.

The directivity patterns for each resonant frequency were plotted in Figure 15 directly while continuously rotating the model 360 deg about its longitudinal or vertical centerline axis. The acceleration distributions already plotted in Figure 14 are shown as dotted lines on Figure 15 in relative decibel levels.

Resonant frequencies having identifiable vibration mode shapes are presented in Figure 16. This figure shows that many modes were either not excited or were unidentifiable by the procedure used.

DISCUSSION

Investigation of the vibrational characteristics was limited to one model and therefore it is impossible to compare it with models of different design and material. The discussion must, therefore, be confined to a comparison of the results with existing theories for mechanical vibrations of cylindrical shells.

MOBILITY

Generally, variation between adjacent peaks of mobility for excitation at low frequencies, Figure 11, is greater than at high frequencies.

TABLE 1

Frequency Correlation of Maximum Acceleration
Mode Shapes and Sound Pressure Directivity Patterns

n	m	1	3	5	7	9
1	VERT	300*†	----	----	----	----
	HORZ	300*†	----	----	----	----
	SPDP	300 †	----	----	----	----
2	VERT	1180	1660	2500	3510	4500*
	HORZ	1180	1660	2500	3510	4500
	SPDP	1160**	1730**	2500/2459††	3440	4500
3	VERT	3050	3260	3760	----	----
	HORZ	3050	3260	3760	----	----
	SPDP	3100	3240/3220††	3670/3680††	----	----
4	VERT	5270	----	----	----	----
	HORZ	5270	----	----	----	----
	SPDP	5270	----	----	----	----

*Run taken at point of maximum acceleration.

**Plot not presented because of poor directivity pattern.

†Bending mode.

††Horizontal orientation.

n = Number of circumferential full waves

m = Number of longitudinal half waves

Frequencies are in cps (all modes are lobar modes unless otherwise noted).

VERT - Model oriented in vertical position (longitudinal axis vertical).

HORZ - Model oriented in horizontal position (longitudinal axis horizontal).

SPDP - Sound pressure directivity patterns (vertical orientation unless otherwise noted).

This can be attributed to the frequency dependent damping mechanism and to the lower strain energy of bending and stretching for less complicated modes.

The average mobility at resonance approached 0.1 in/lb-sec (10 lb/in/sec impedance), which is in good agreement with the values measured on GRP foundations by Westinghouse Research Laboratories.[4]

An estimate of damping can be obtained from the acceleration response curve of Figure 12 by calculating the quality factor Q and the loss tangent η

$$Q = \frac{F_n}{\Delta f} \frac{\sqrt{(A_R)^2 - (A)^2}}{A^2}$$

where

Q = quality factor

F_n = resonant frequency

Δf = bandwidth

A_R = amplification factor of the peak

A = amplification factor at desired bandwidth

η = loss tangent $= \frac{1}{Q} = 2 \frac{C}{C_c}$

C/C_c = ratio between damping and critical damping

The range of Q is from 90 at the sharpest resonance (1190 cps) to 15 at the apparent broadest resonance (1960 cps) with C/C_c varying from 0.5 to 3.5 percent.

VIBRATION MODE SHAPES

The mode shapes in Figure 14 were obtained by the phase separation technique of Stahle.[5] Stahle makes three basic assumptions: (1) at resonance the mobility is primarily damping-controlled and the acceleration will be in quadrature with the force; (2) the off-resonant modes are all either in-phase or 180° out-of-phase with the driving force thus not contributing to the acceleration response; and (3) very light damping. These assumptions are valid only if sufficient separation exists between resonances.

Figure 15 presents a comparison between absolute values of the vibration mode shapes and corresponding directivity patterns at resonant

frequencies. The circumferential acceleration follows a cos $n\psi$ distribution and many of the sound pressure directivity patterns show a correspondence with the acceleration distribution. Table 1 is a tabulation of frequencies with maximum acceleration and corresponding directivity patterns.

Figure 16 shows that an increase of the excitation frequency excites more complex mode shapes. This is in agreement with experiments made by Arnold and Warburton[6] on steel cylinders with various plate thickness and their experimental curves for free-free end conditions with rigid end-caps. The inability to identify many of the higher mode shapes excited at resonance limits the curves of Figure 16. The absence of even-numbered "m" is to be expected since the drive point was centrally located and, therefore, at a nodal point for even m's.

All observed modes shapes had an antinode at the drive point indicating that the model was completely homogeneous and that none of the mode shapes took up a preferential nodal position due to stress concentrations or construction discontinuities. This was expected since the plastic filament-wound model has no welded joints or locked-in stress concentrations due to forming processes. On the other hand, experiments on cylinders of steel construction have been known to have more than one resonant frequency for a single mode shape (n, m), i.e., the nodal rings generated by the longitudinal vibrations and the nodal lines generated by the circumferential vibrations take different preferential locations.

SOUND PRESSURE LEVELS

A very good agreement of maximum mobility and maximum sound pressure level at corresponding frequencies is shown by comparing peaks of mobility, Figure 11, with those of sound pressure level, Figure 13. The minor discrepancies in frequency are attributed to the two separate automatic recording systems used for mobility and sound pressure level measurements.

According to theory, sound pressure levels should increase with increasing frequency. This is not apparent in Figure 13 because of the characteristics of the shaker.

DIRECTIVITY PATTERNS

The directivity patterns for each resonant frequency were obtained for both vertical and horizontal orientation of the longitudinal axis.

For frequencies above 200 cps the test setup satisfies the conditions for a free field. For frequencies above 1000 cps the hydrophone, at two meters, was at least 1 wavelength distance away from the sound projector to be in the far field. Two meters were chosen as a compromise between low-signal levels and near-field distortions.

The directivity patterns, Figure 15, show decided directionality. For the vertical orientation, the cos $n\psi$ acceleration distribution is plotted (dotted line) and shows an interesting correlation between acceleration decibel (re 1 mv) and sound pressure level in decibel (re 0.0002 μ bar). Brighman and Borg[7] have shown that this will be the case for a finite cylinder in the far field.

For horizontal orientation the directivity pattern is essentially 2-lobed with longitudinal lobar modes superimposed, such as shown in Figures 15c, 15h, and 15j.

INSTRUMENTATION LIMITATIONS

Test results were somewhat limited by the available instrumentation:

1. The shaker output for a constant voltage input decreased with increasing frequency.

2. No filtering was available so that the acceleration response at antiresonances is obscured by the amplifier noise level.

3. The separate systems used for mobility and sound pressure level measurements were not compatible, resulting in minor discrepancies of resonant frequencies.

4. Phase angle recordings, such as Figure 12, made during frequency sweeps were in general disregarded because of noise interference, no tracking filters, and no signal amplitude control for the phase meter inputs.

5. Water seepage into the model and instrumentation made several recordings questionable, especially for higher frequencies, and they were therefore discarded.

CONCLUSIONS

1. As the frequency increases the mobility at resonance approaches a value of 0.1 in/lb-sec with an average mobility of 0.05 in/lb-sec.

2. At most resonant frequencies the vibration mode shapes and associated sound directivity patterns were determined around the circumference of the model, and there is good agreement between vibration mode shapes and sound directivity patterns around the circumference of the model. The sound directivity pattern in the plane of the longitudinal axis was 2-lobed with superimposed lobar modes.

3. The range of damping was from 0.5 to 3.3 percent C/C_c with Q ranging from 15 to 90.

4. For higher modes, above n = 4 and m = 9, vibration mode shapes and directivity patterns could not be identified.

5. Sound pressure levels over the measurement frequency range (200 to 5300 cps) varied from 80 to 115 db (re 0.0002 μ bar/2 meters).

6. For plastic material, models with comparatively small dimensions will give satisfactory results. This eliminates the necessity of using elaborate test sites with great water depth, and thereby reduces considerably the cost of experiments.

7. Glass-reinforced models exhibit considerable construction homogeneity; therefore, better agreement can be obtained between theory and experimental model test results.

8. Semiautomatic instrumentation, and unreliable components, limited evaluation of test data and increased test time. It should be replaced with fully automatic instrumentation for future tests.

RECOMMENDATIONS

Mobility and sound pressure tests for additional plastic models of desirable construction should be continued, and results should be compared with each other and with a model of steel construction.

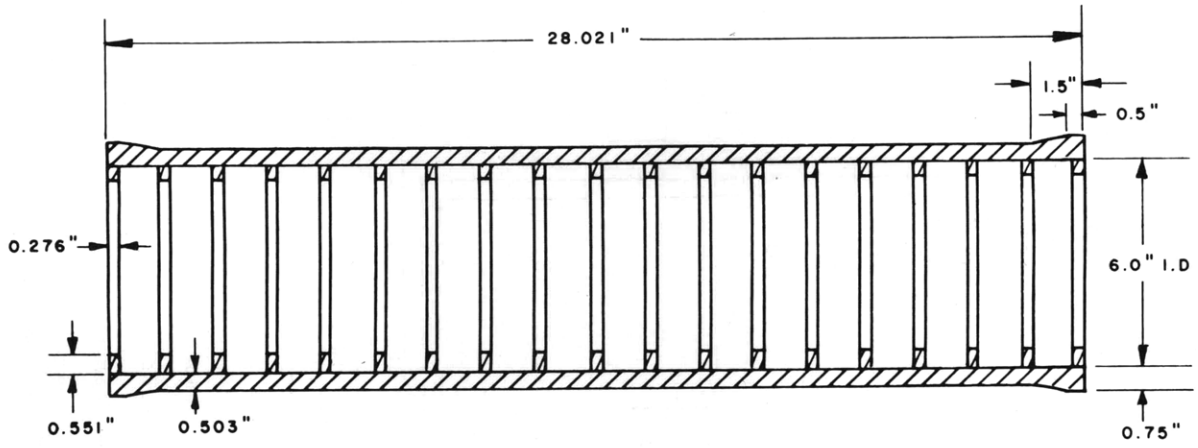

Figure 1 – Details of Glass-Reinforced-Plastic Test Model, RV-8

Material: U.S. Polymecic HTS E-787 Pre Preg.

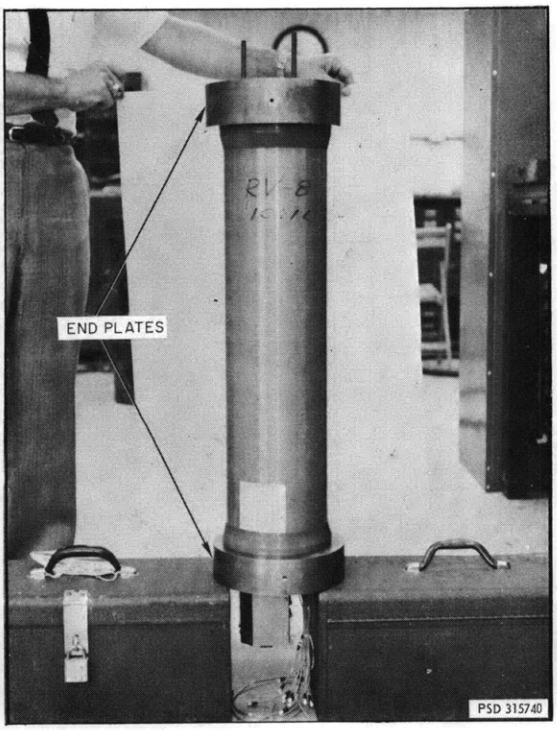

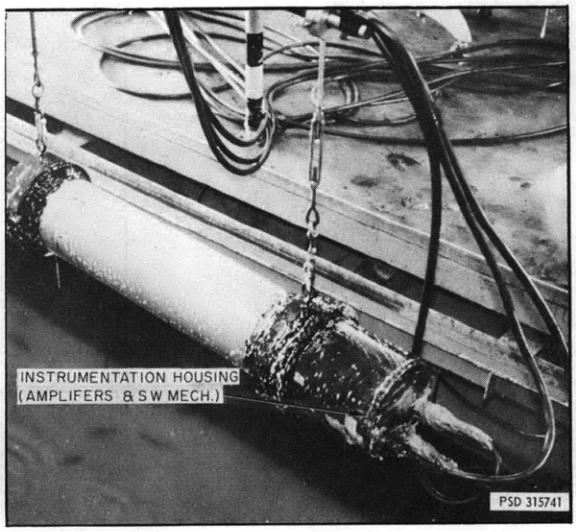

Figure 2b

Figure 2 – Photographs of Glass-Reinforced-Plastic Test Model, RV-8

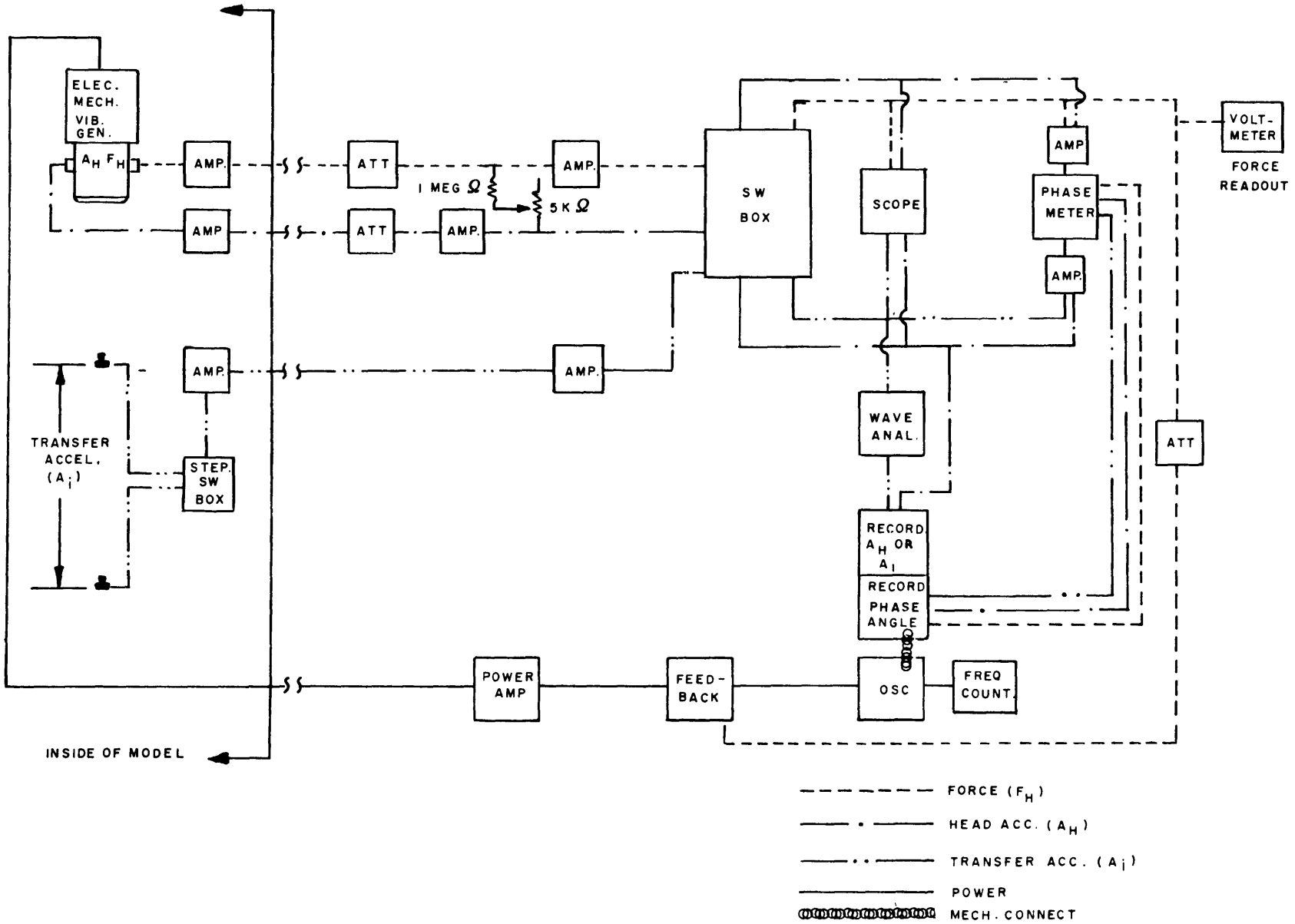

Figure 3 – Block Diagram of Mechanical Mobility Measuring System

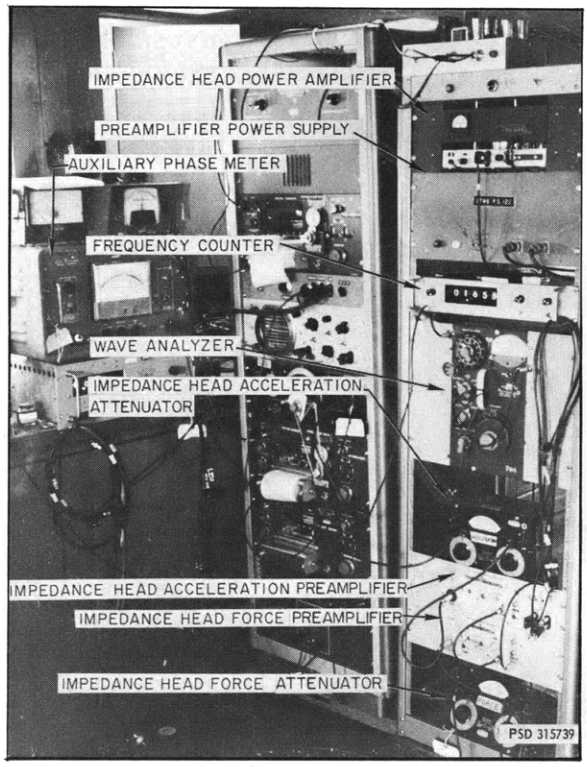

Figure 4a

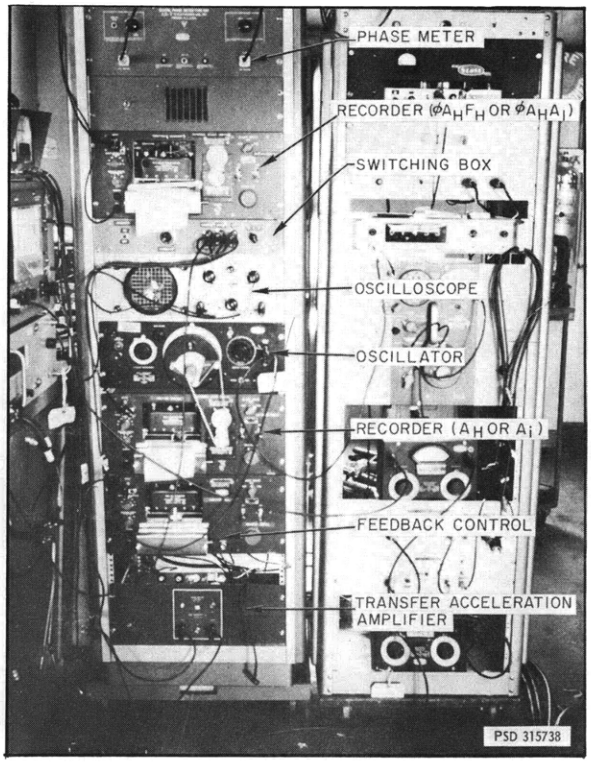

Figure 4b

Figure 4 – Photograph of TMB Mobility Measuring System

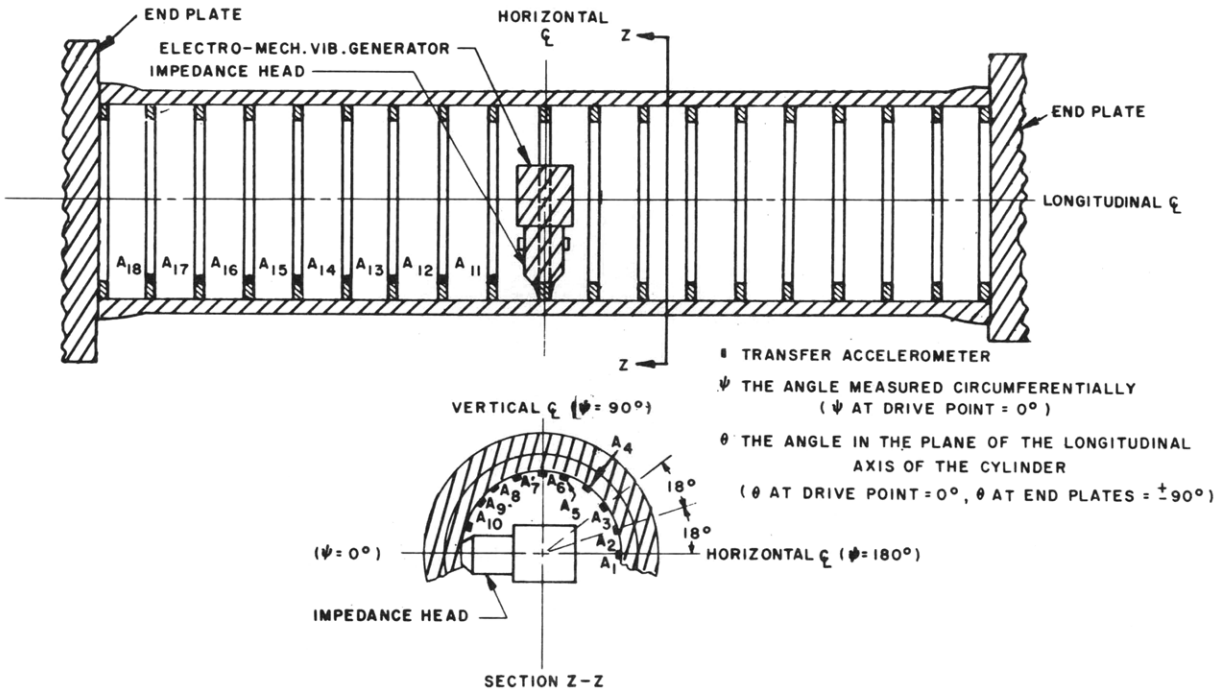

Figure 5 – Measuring Positions Inside the Model

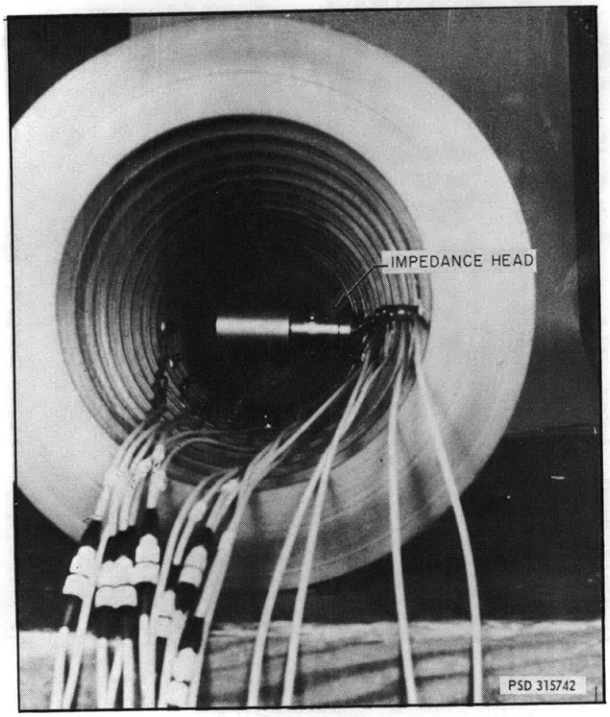

Figure 6a

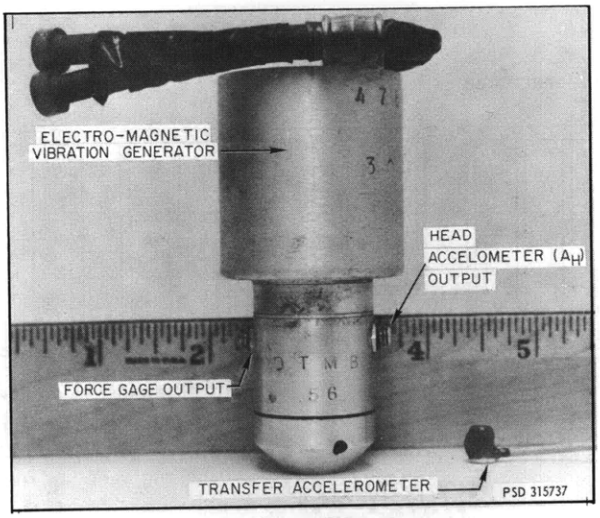

Figure 6b

Figure 6 – Photographs of Model Instrumentation

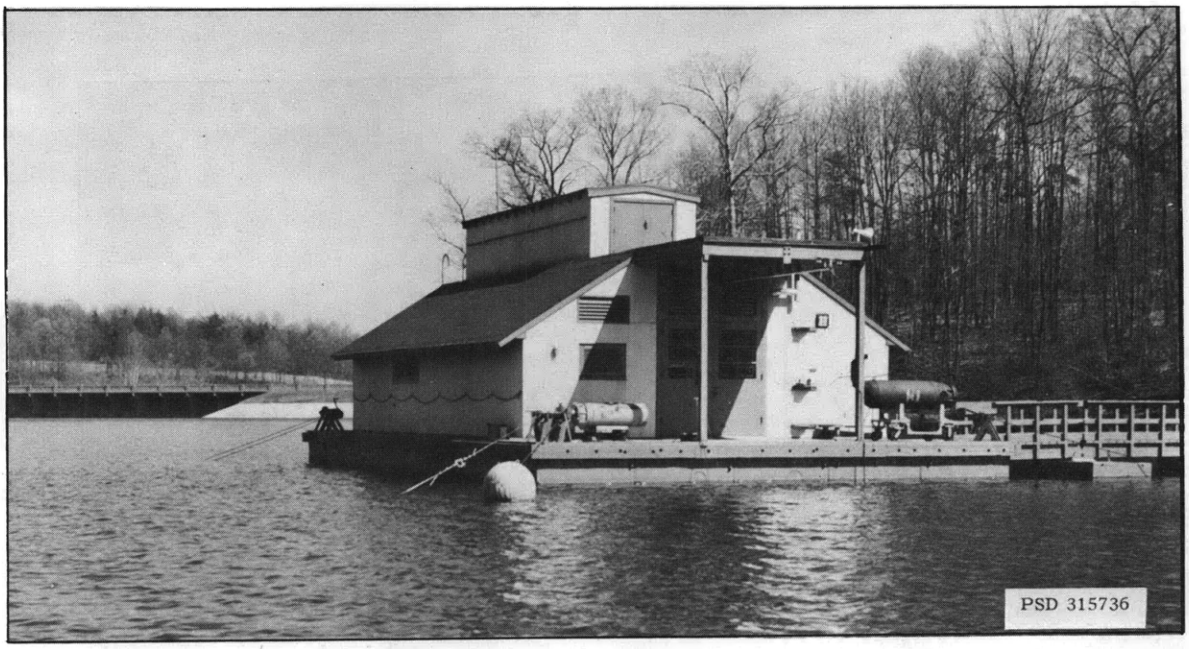

Figure 7a – Photographs of the Naval Ordnance Laboratory Facility

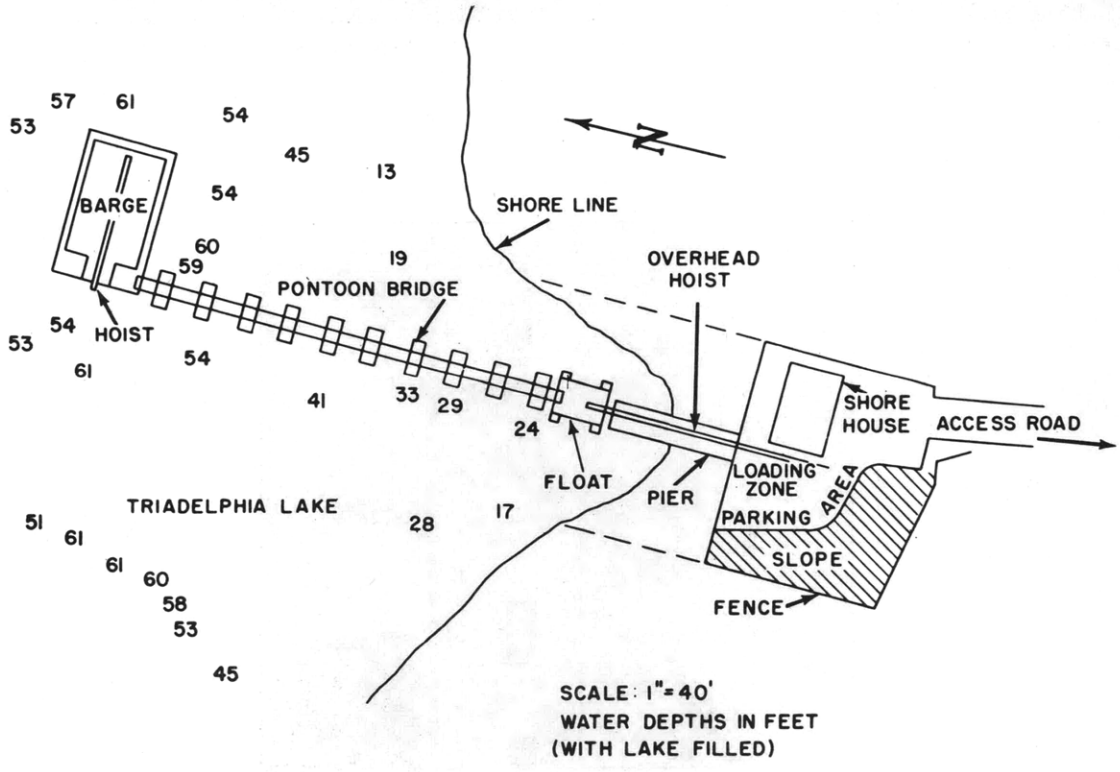

Figure 7b – Sketch Showing General Layout at Naval Ordnance Laboratory Facility

Figure 7 – Naval Ordnance Laboratory Acoustic Facility, Physical Plant

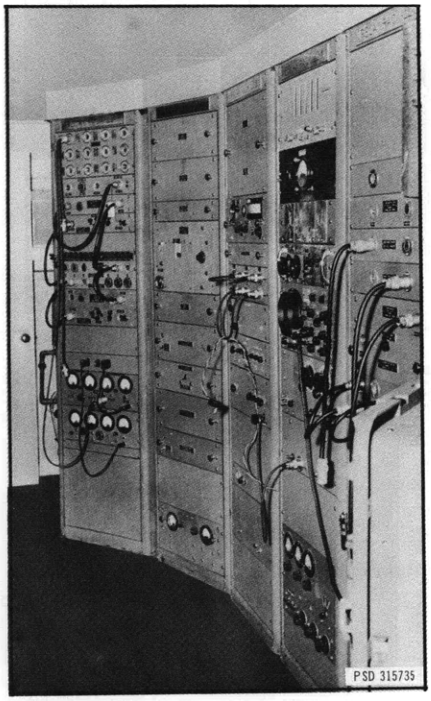

Figure 8a – Low Level Racks

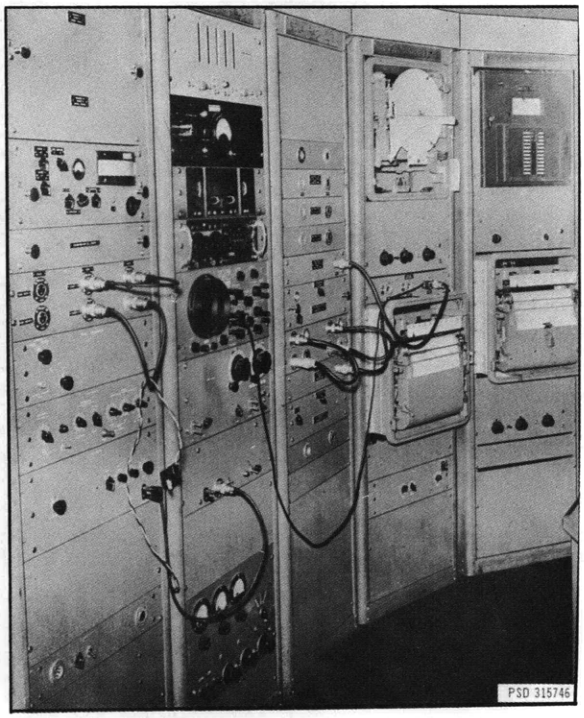

Figure 8b – Low Level Racks

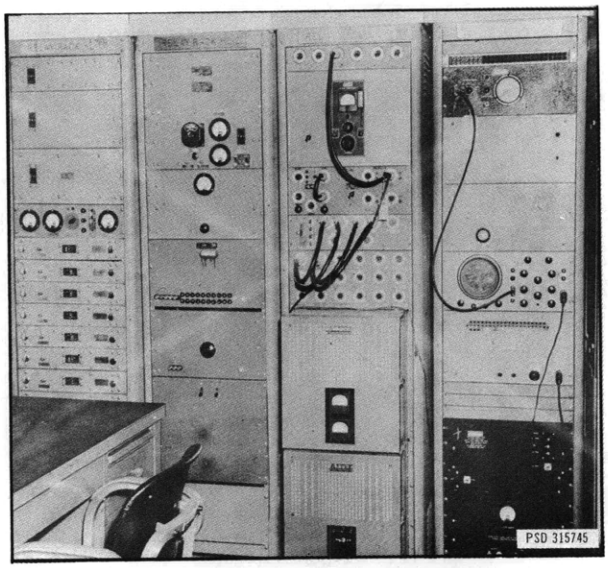

Figure 8c – High Level Racks

Figure 8 – Photographs of Sound Pressure Level Measuring Instrumentation

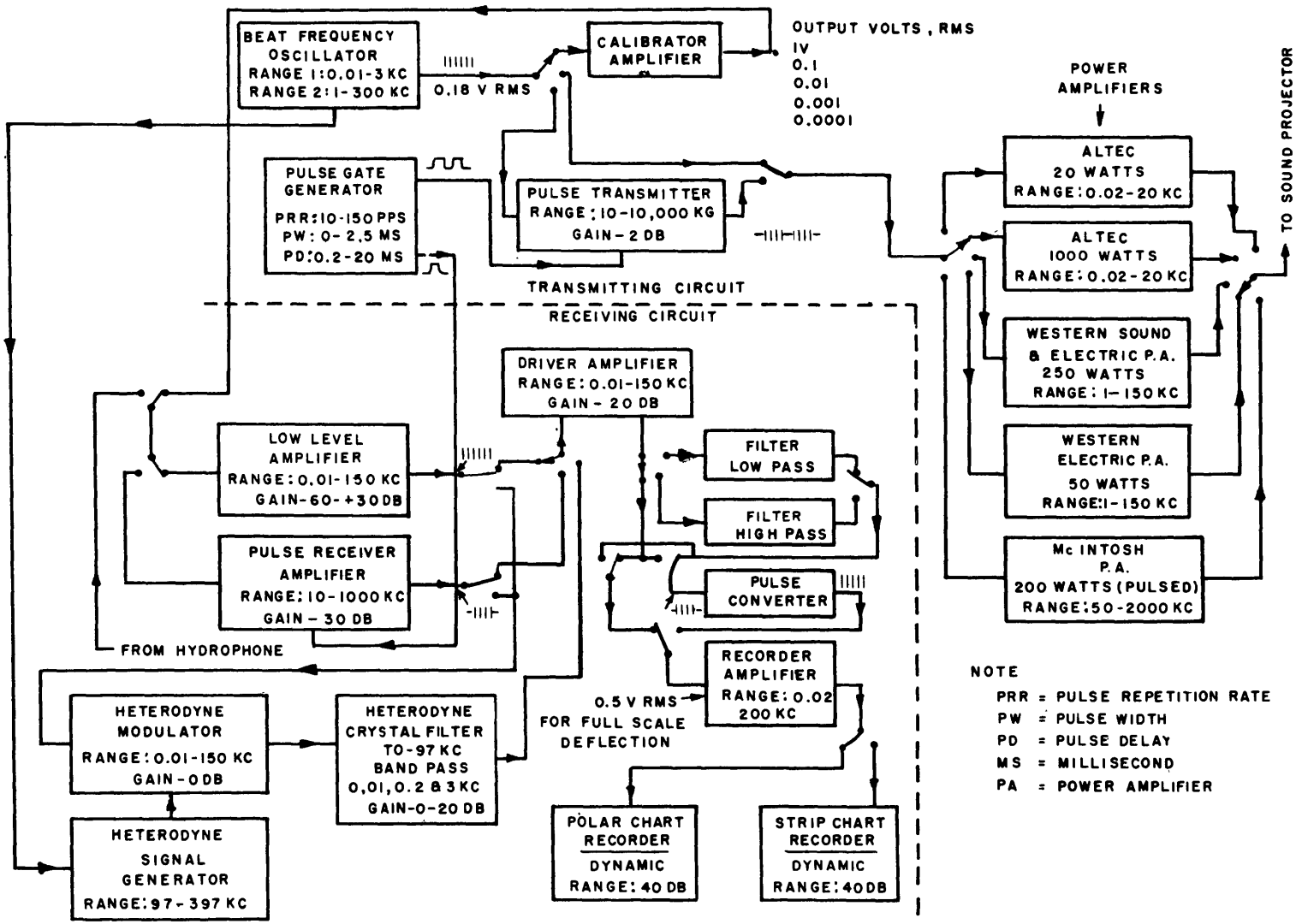

Figure 9 – Block Diagram of Sound Pressure Level Measuring System

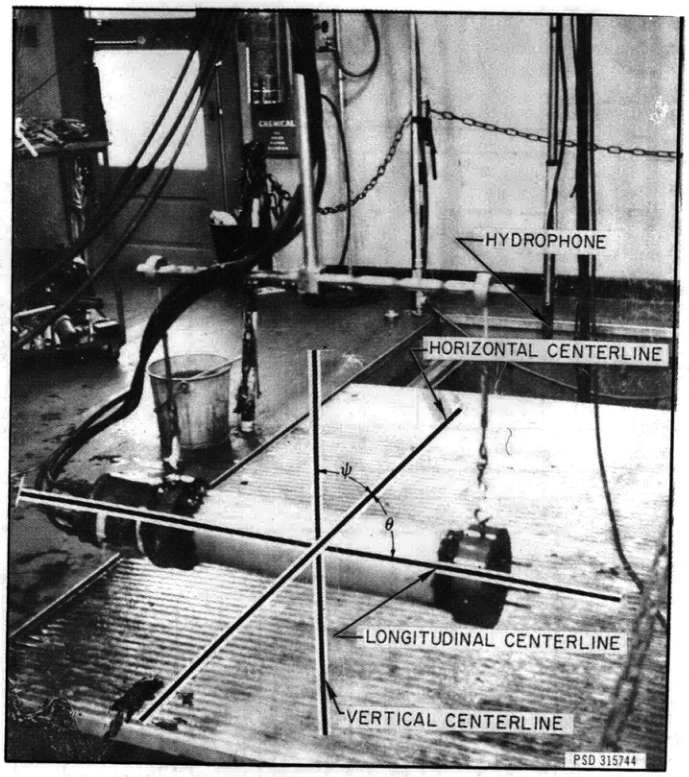

Figure 10a – Model RV-8 Mounted on Suspension System

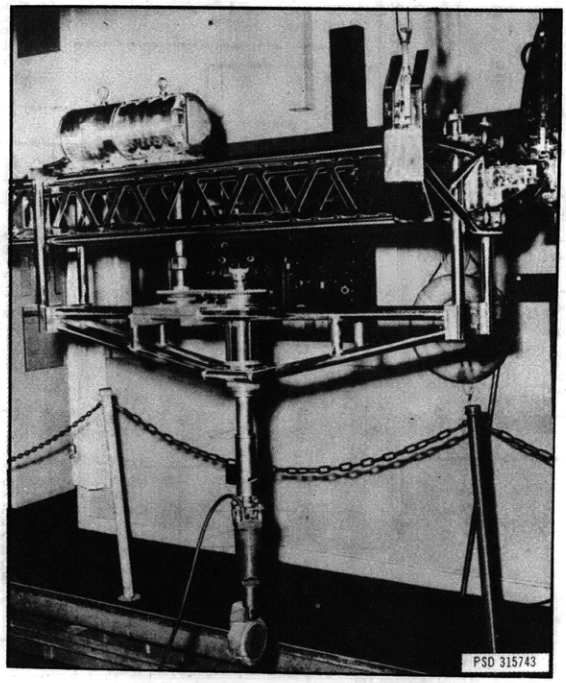

Figure 10b – Rotation Mechanism

Figure 10 – Model Suspension System at Test Site

Figure 11 – Mobility versus Frequency

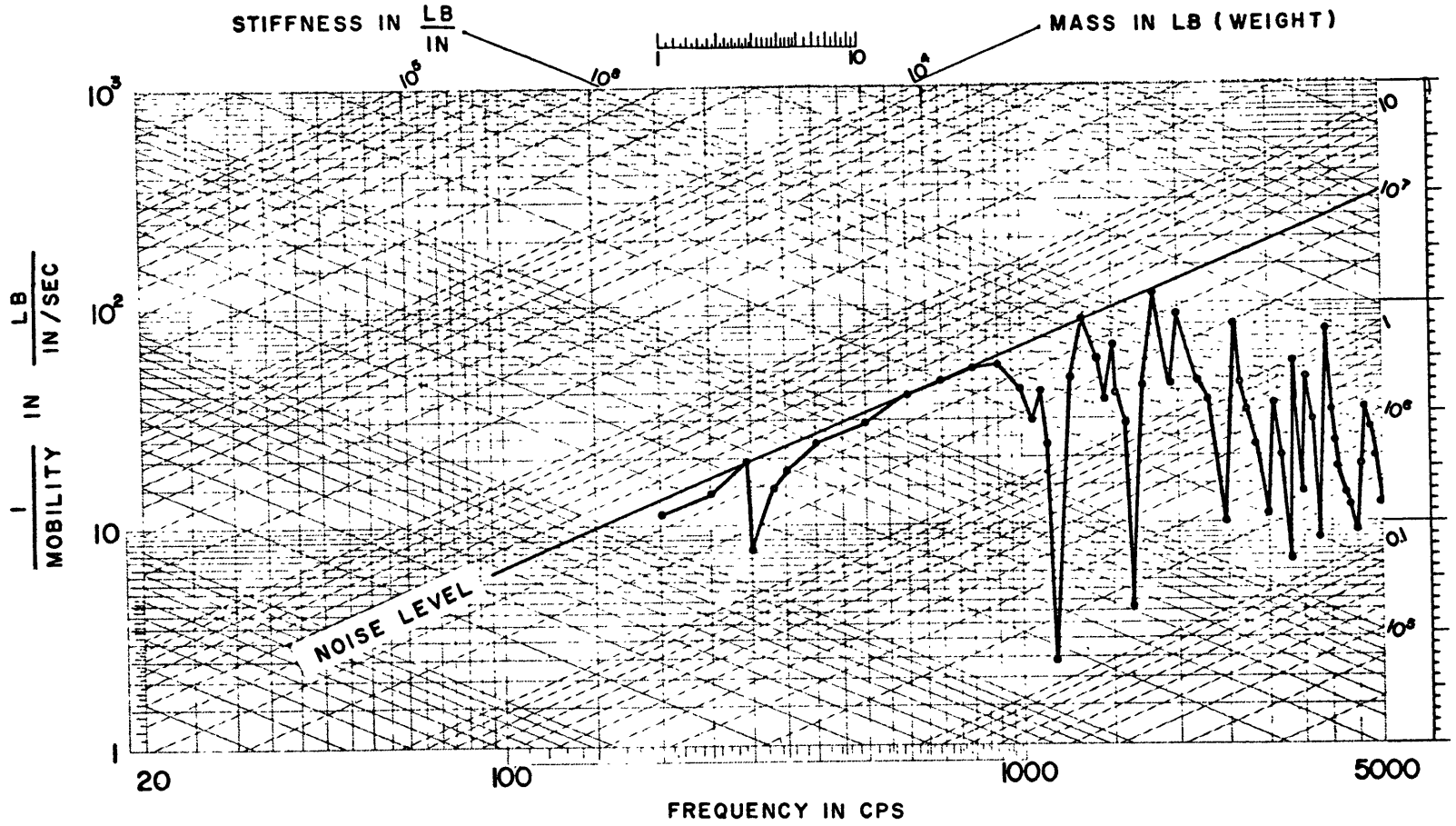

Figure 11a – Mobility versus Frequency, Model Vertical

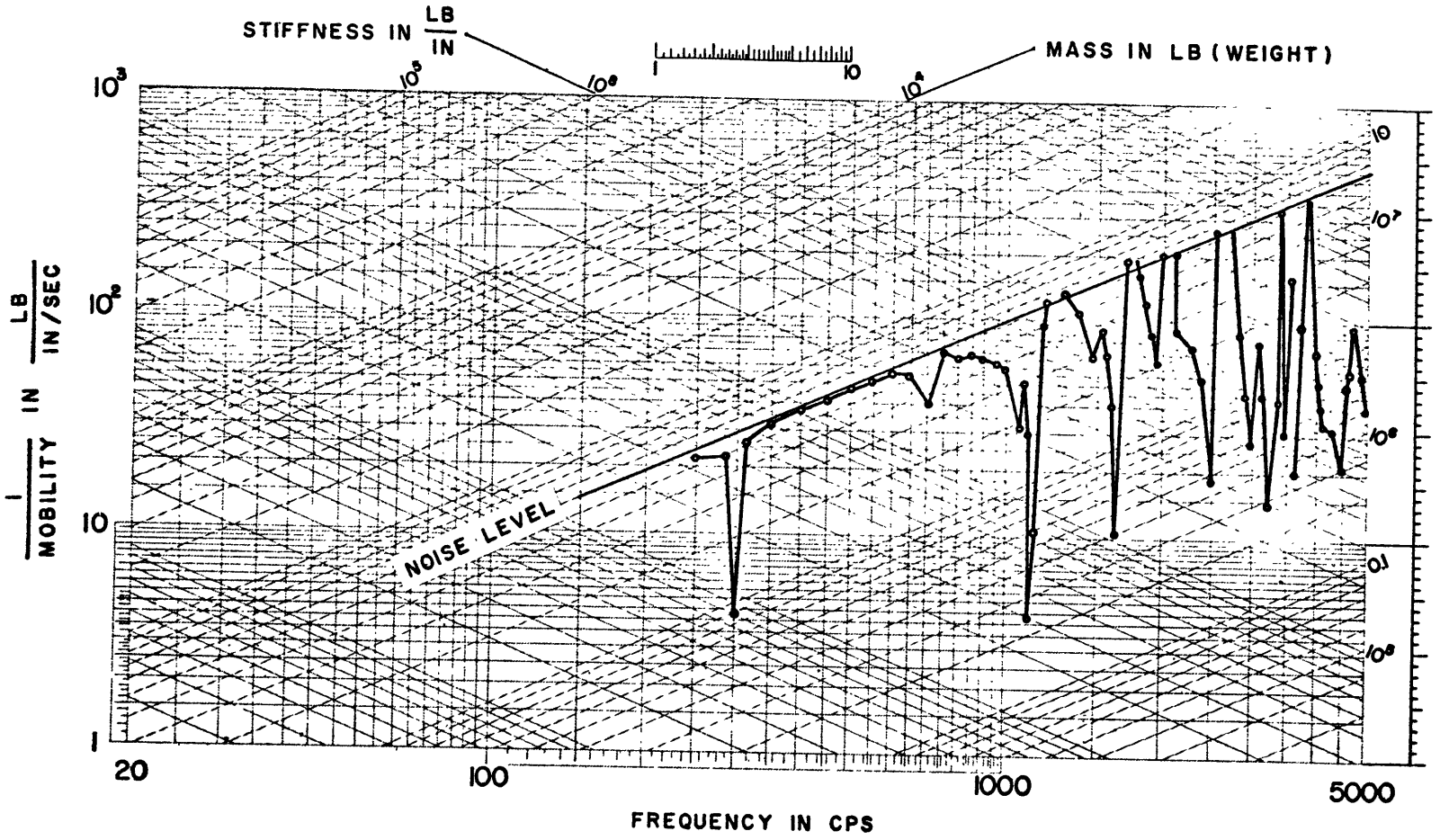

Figure 11b — Mobility versus Frequency, Model Horizontal

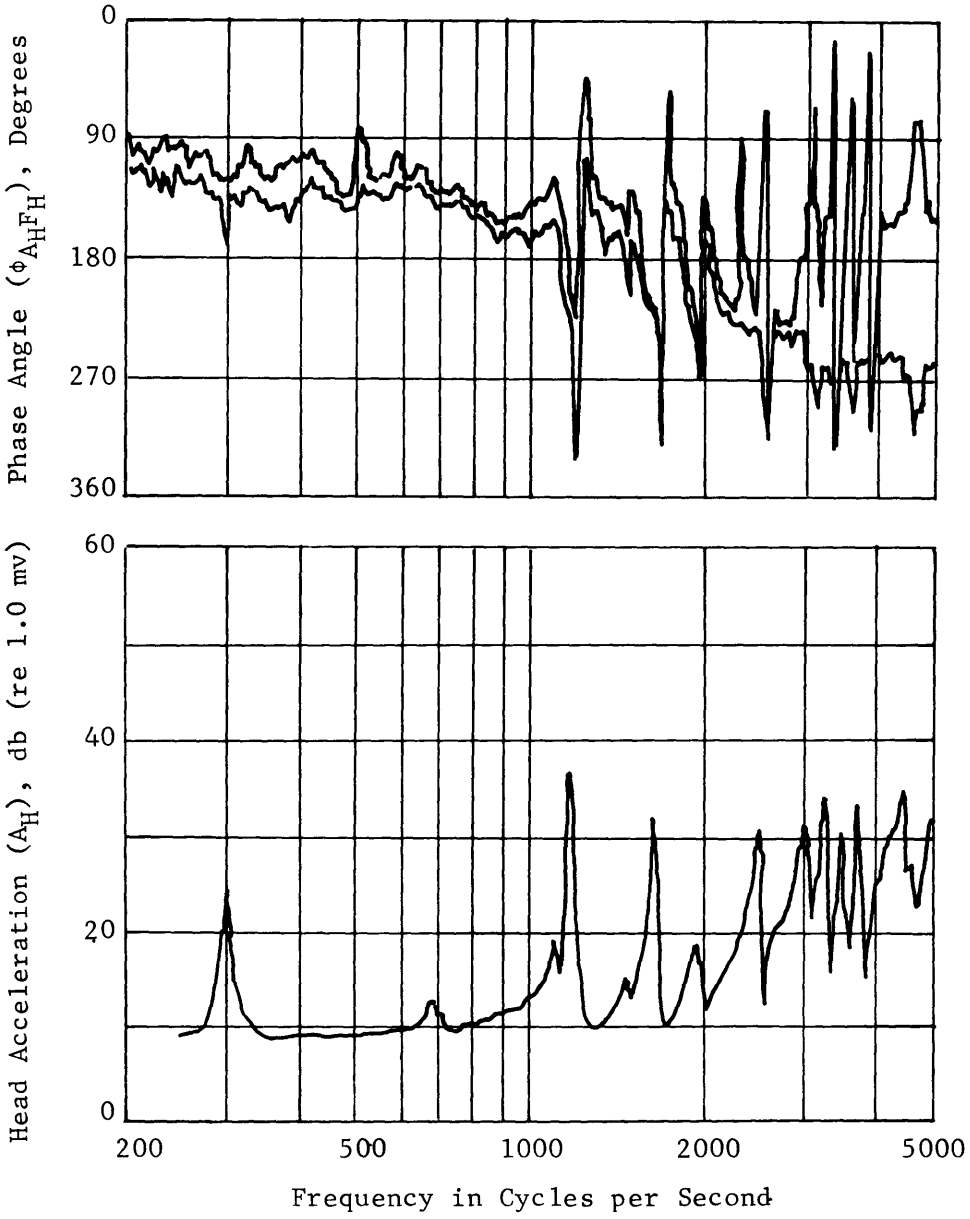

Figure 12 – Sample of Continuous Head Acceleration (A_H) and Phase Angle ($\phi_{A_H F_H}$)

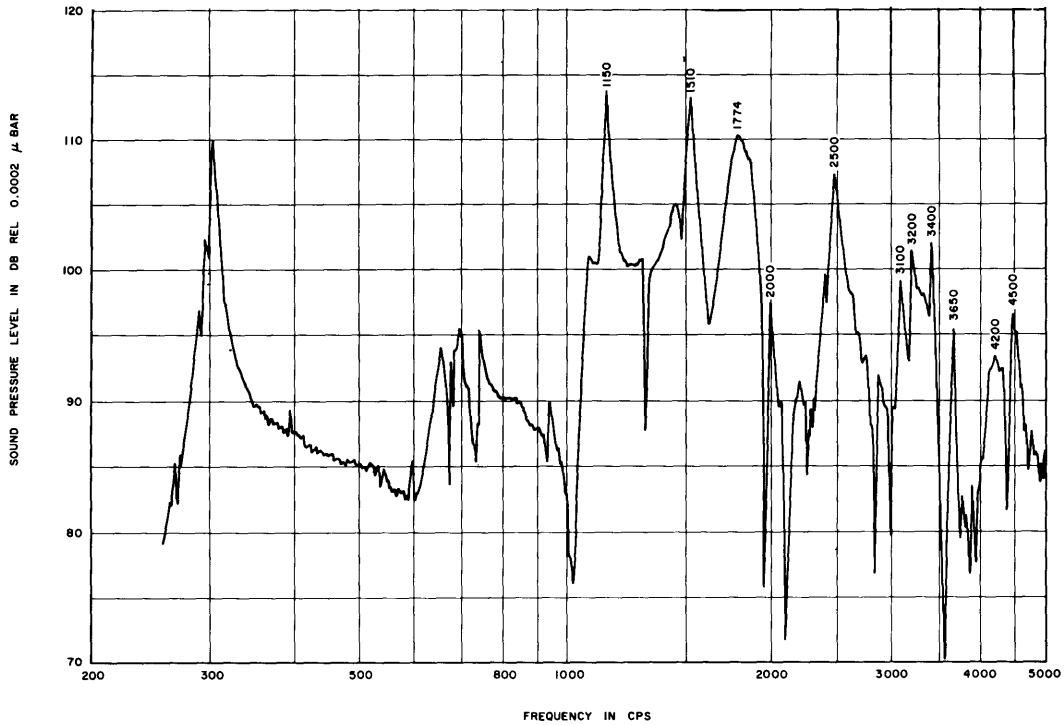

Figure 13a — Model Vertical

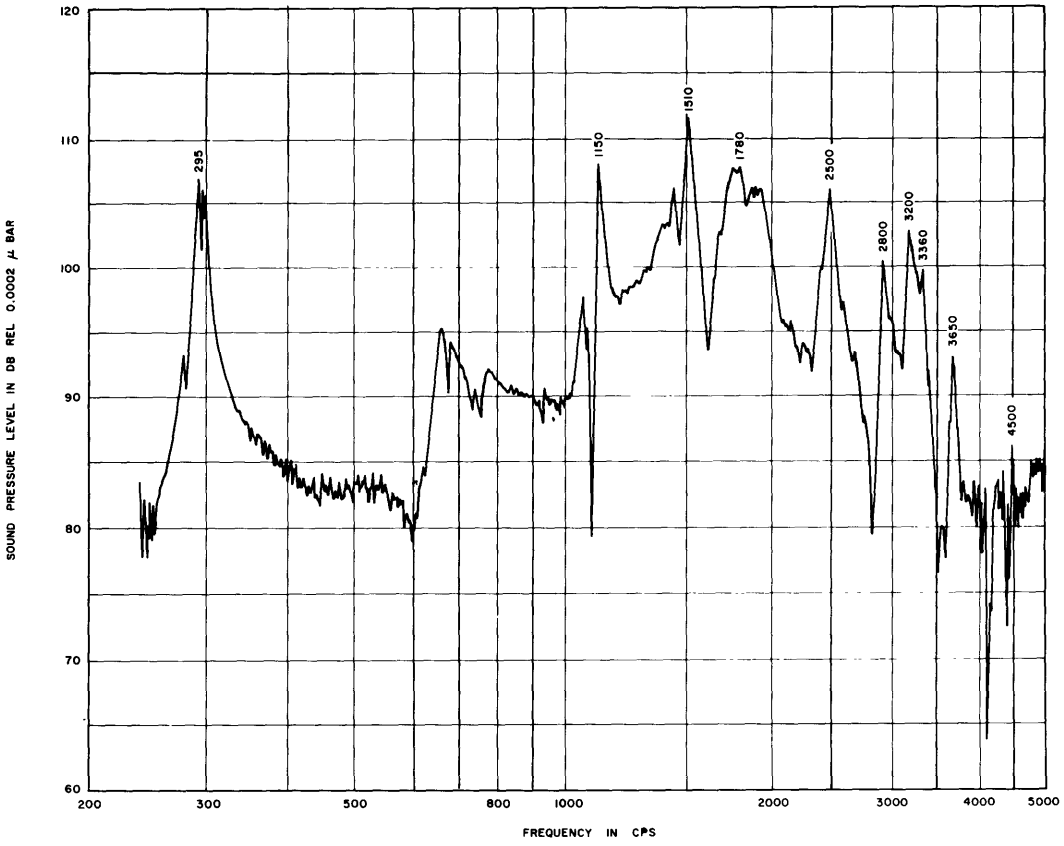

Figure 13b — Model Horizontal

Figure 13 — Sound Pressure Level versus Frequency

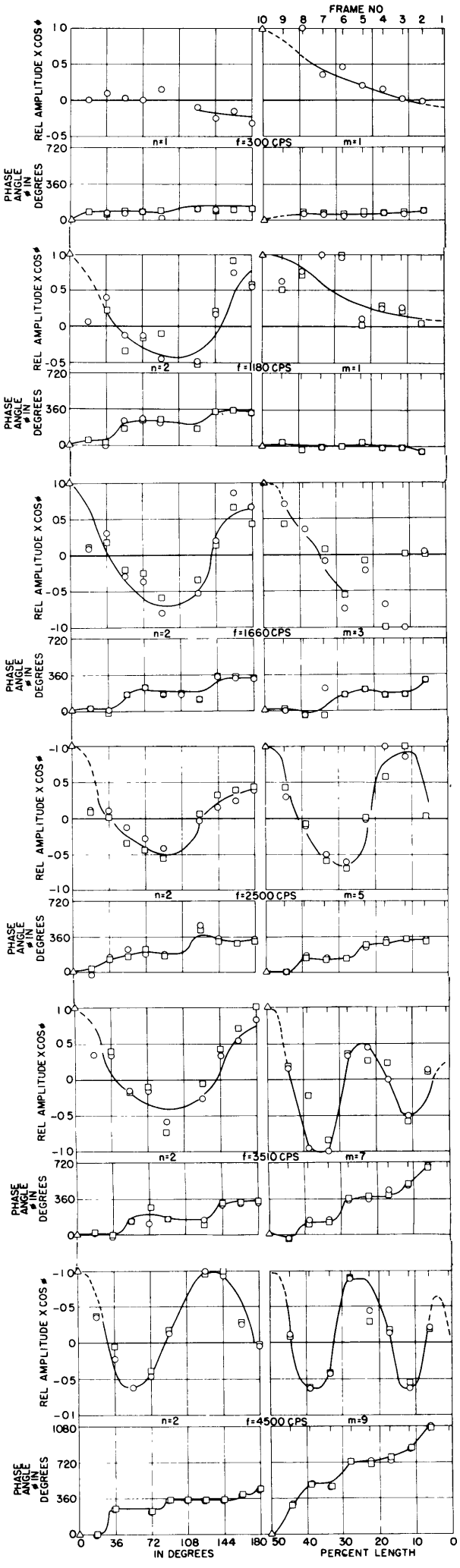

Figure 14a

HORIZONTAL RUN

VERTICAL RUN

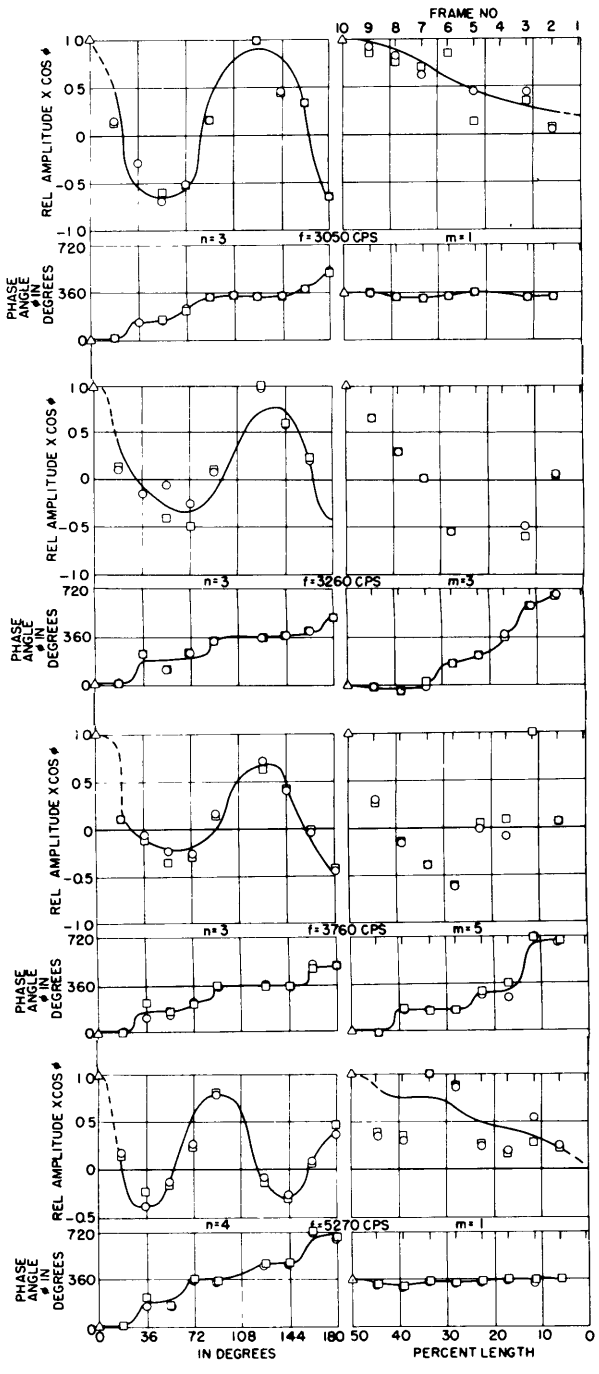

Figure 14b

Figure 14 – Acceleration Distribution at Resonant Frequencies

Figure 15 – Directivity Pattern and Corresponding Acceleration Distribution at Resonant Frequencies

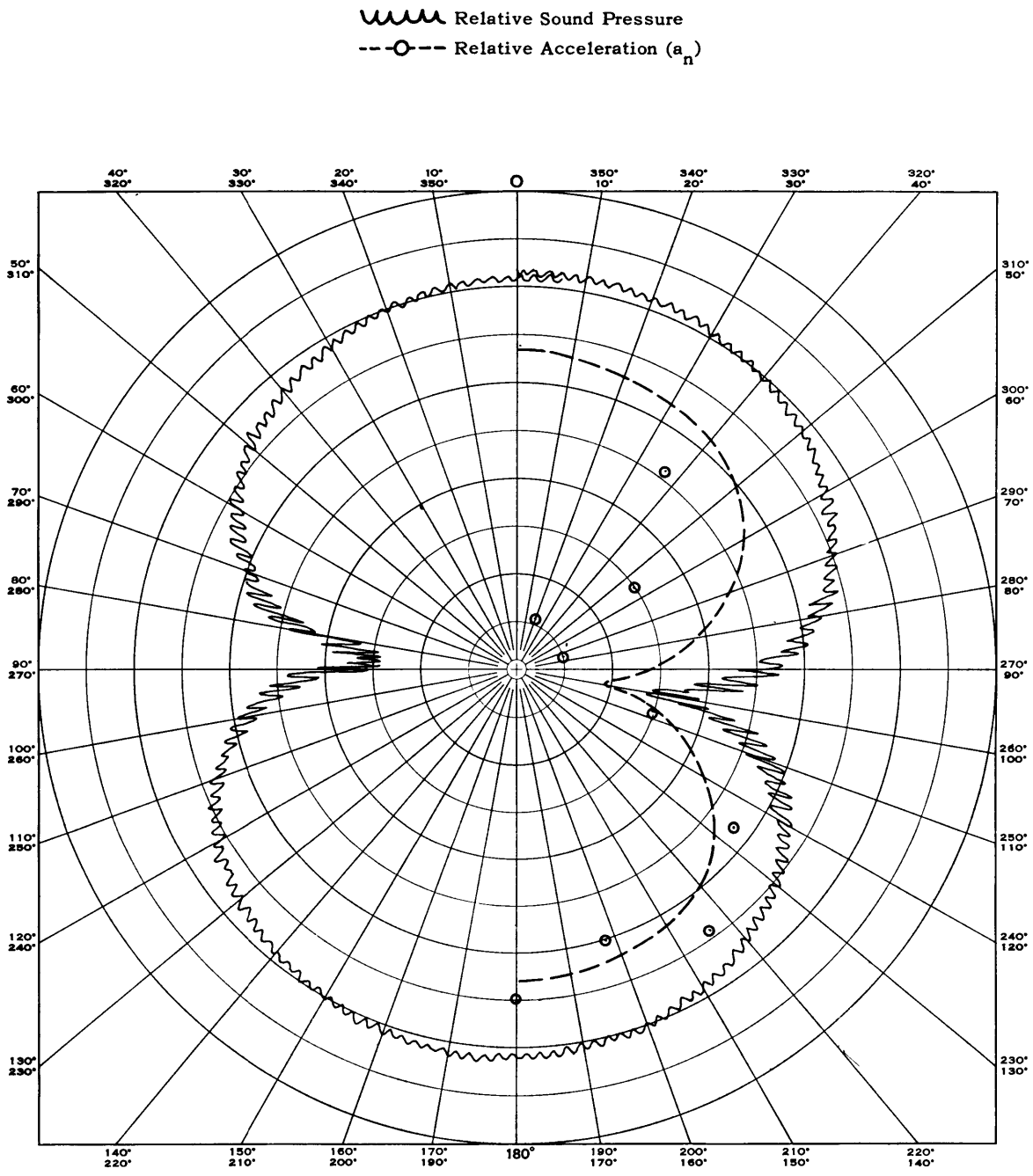

Figure 15a – Model Vertical (n = 1, m = 1) 300 CPS

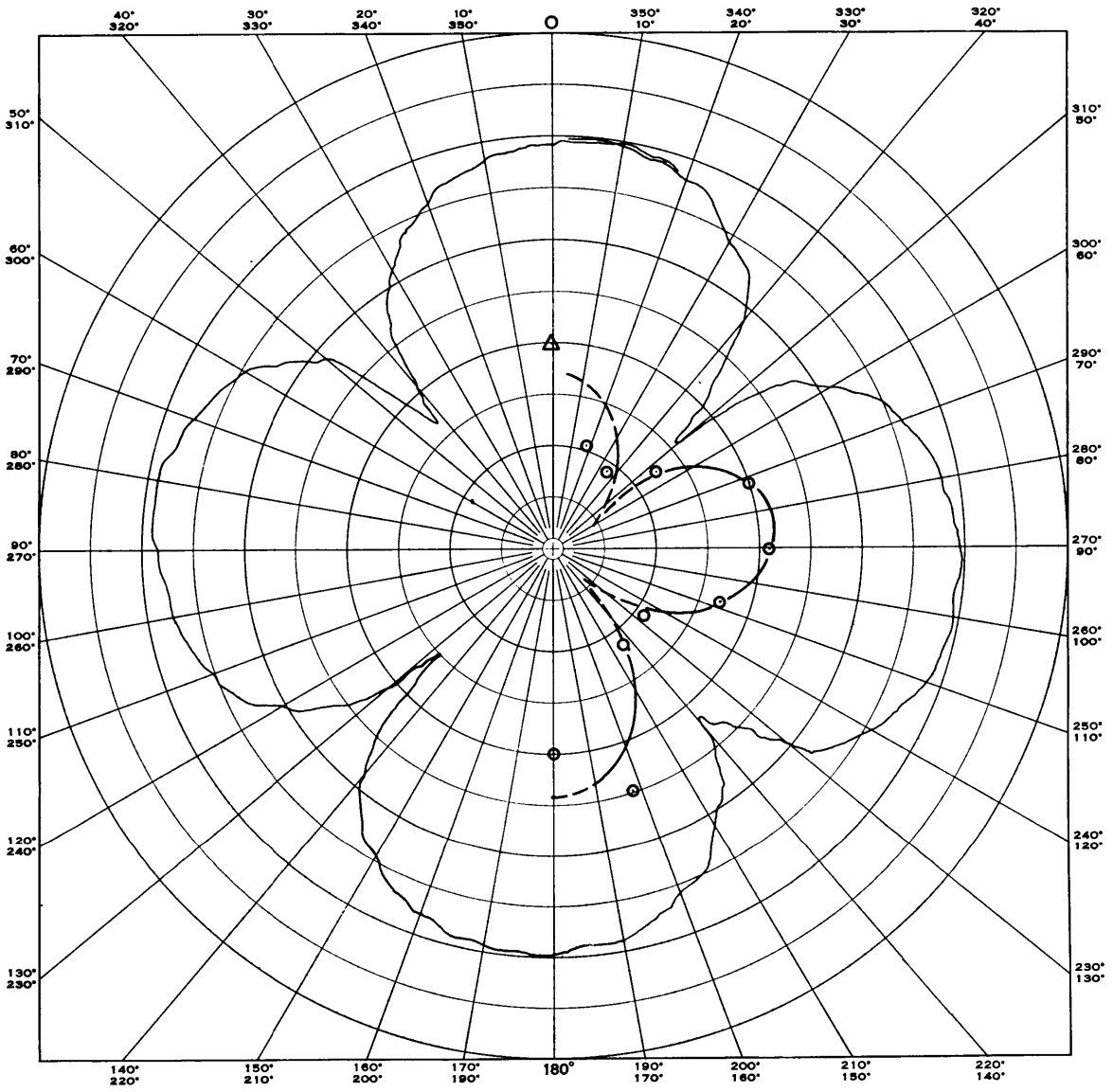

Figure 15b -- Model Vertical (n = 2, m = 5) 2500 CPS

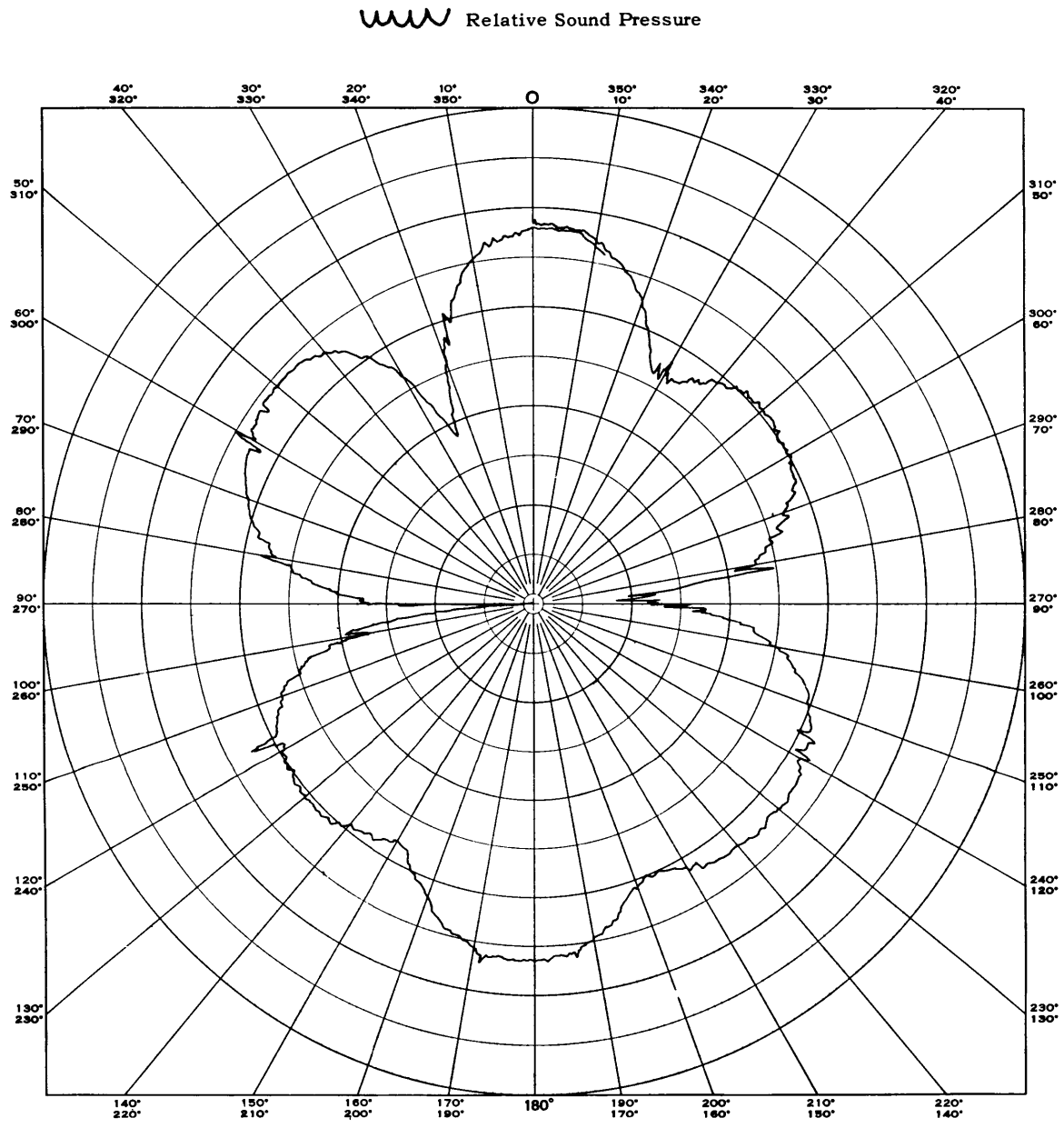

Figure 15c – Model Horizontal (n = 2, m = 5) 2459 CPS

DISTANCE FROM GEOMETRIC CENTER OF MODEL TO HYDROPHONE—7 METERS

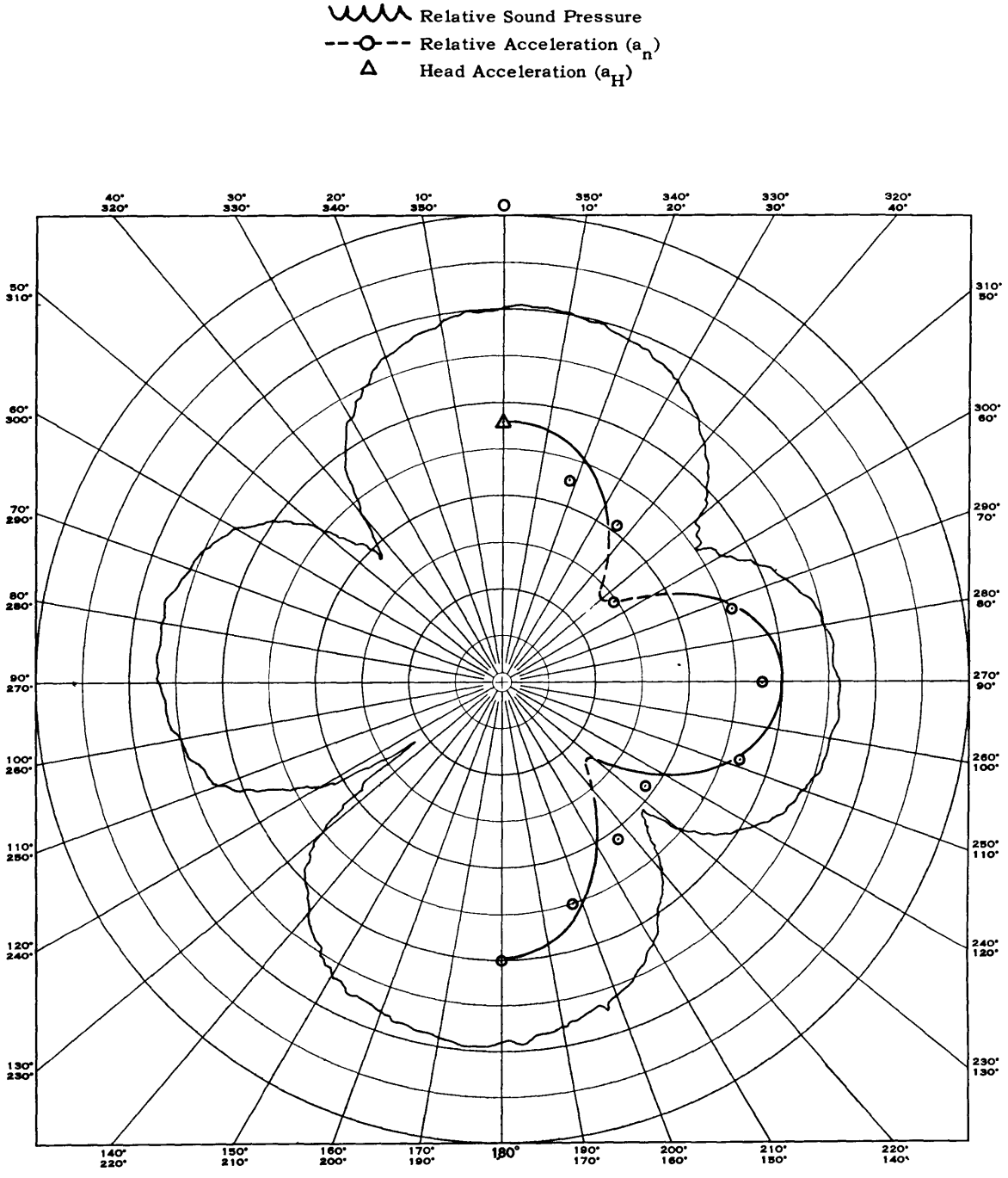

Figure 15d – Model Vertical (n = 2, m = 7) 3440 CPS

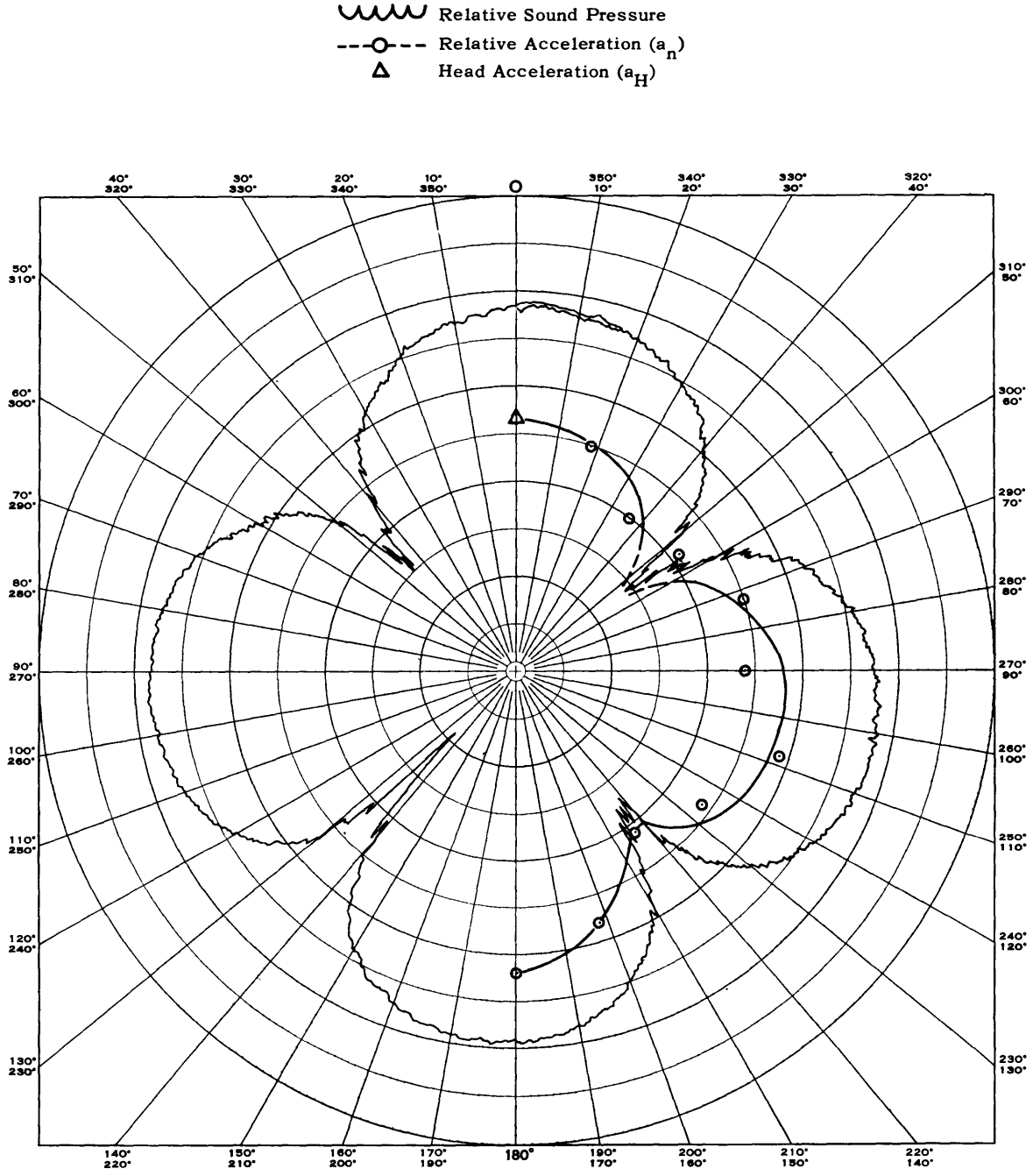

Figure 15e — Model Vertical (n = 2, m = 9) 4500 CPS

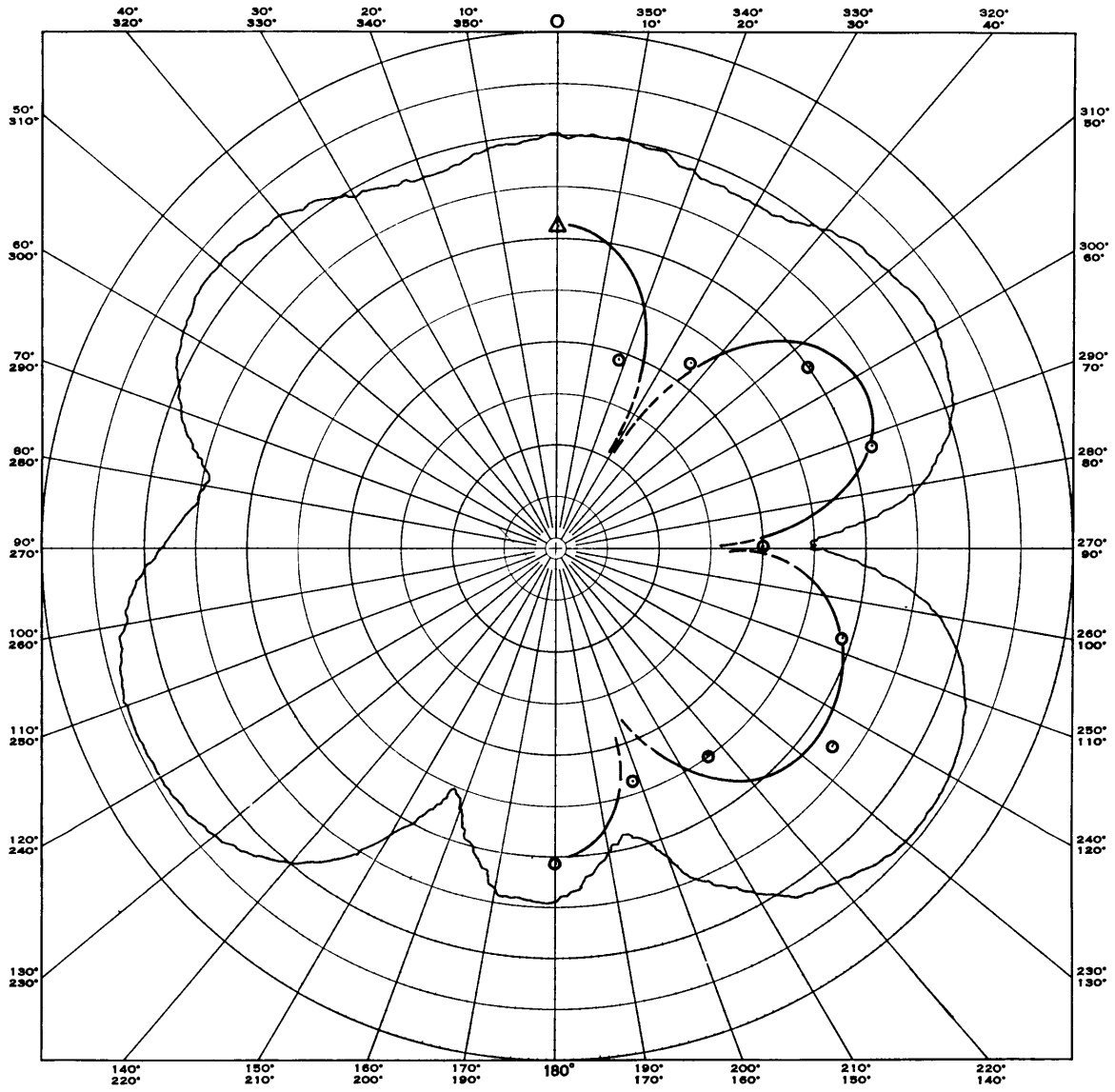

Figure 15f – Model Vertical (n = 3, m = 1) 3100 CPS

Relative Sound Pressure
Relative Acceleration (a_n)
Head Acceleration (a_H)

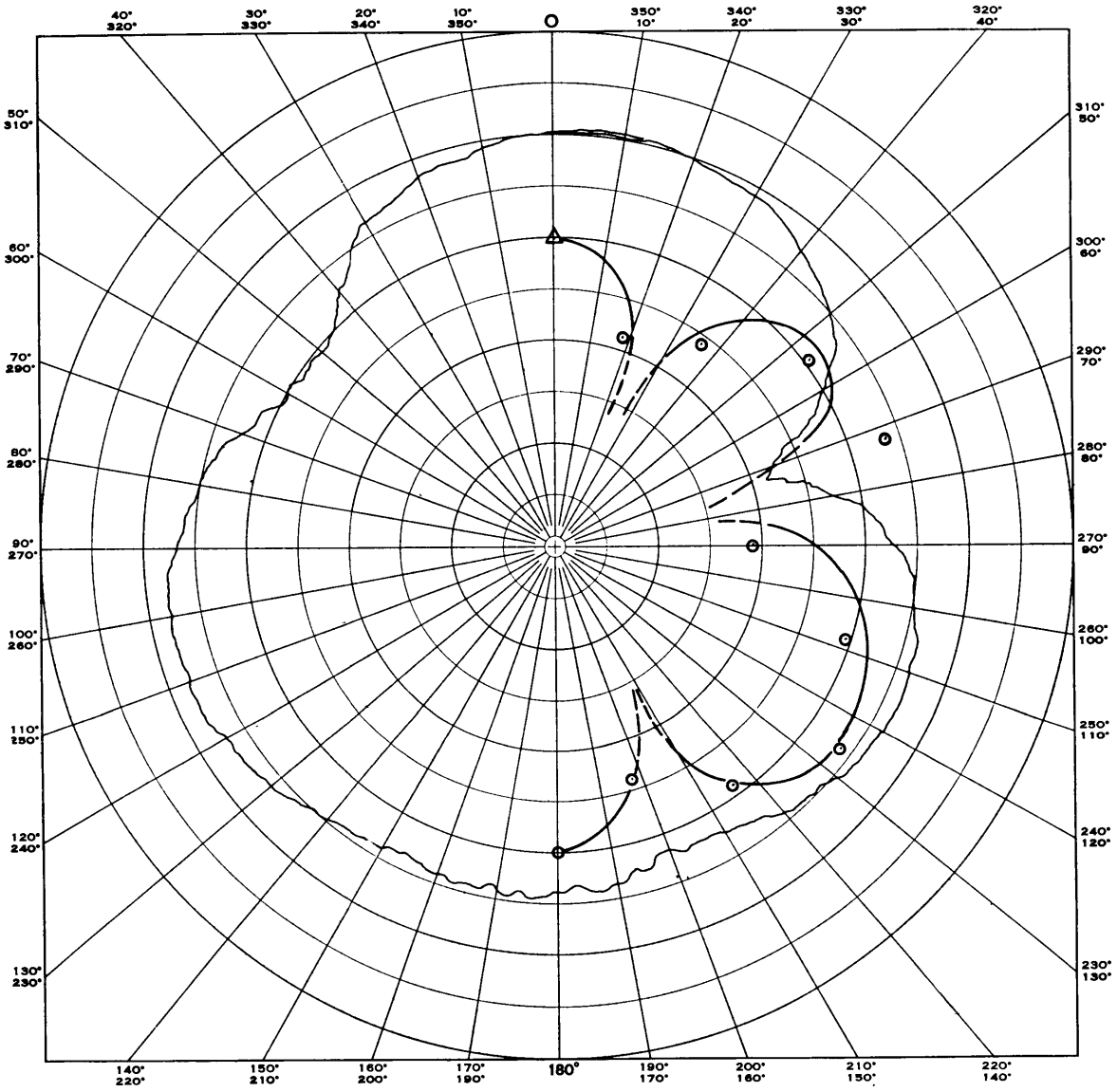

Figure 15g ⊥ Model Vertical (n = 3, m = 3) 3240 CPS

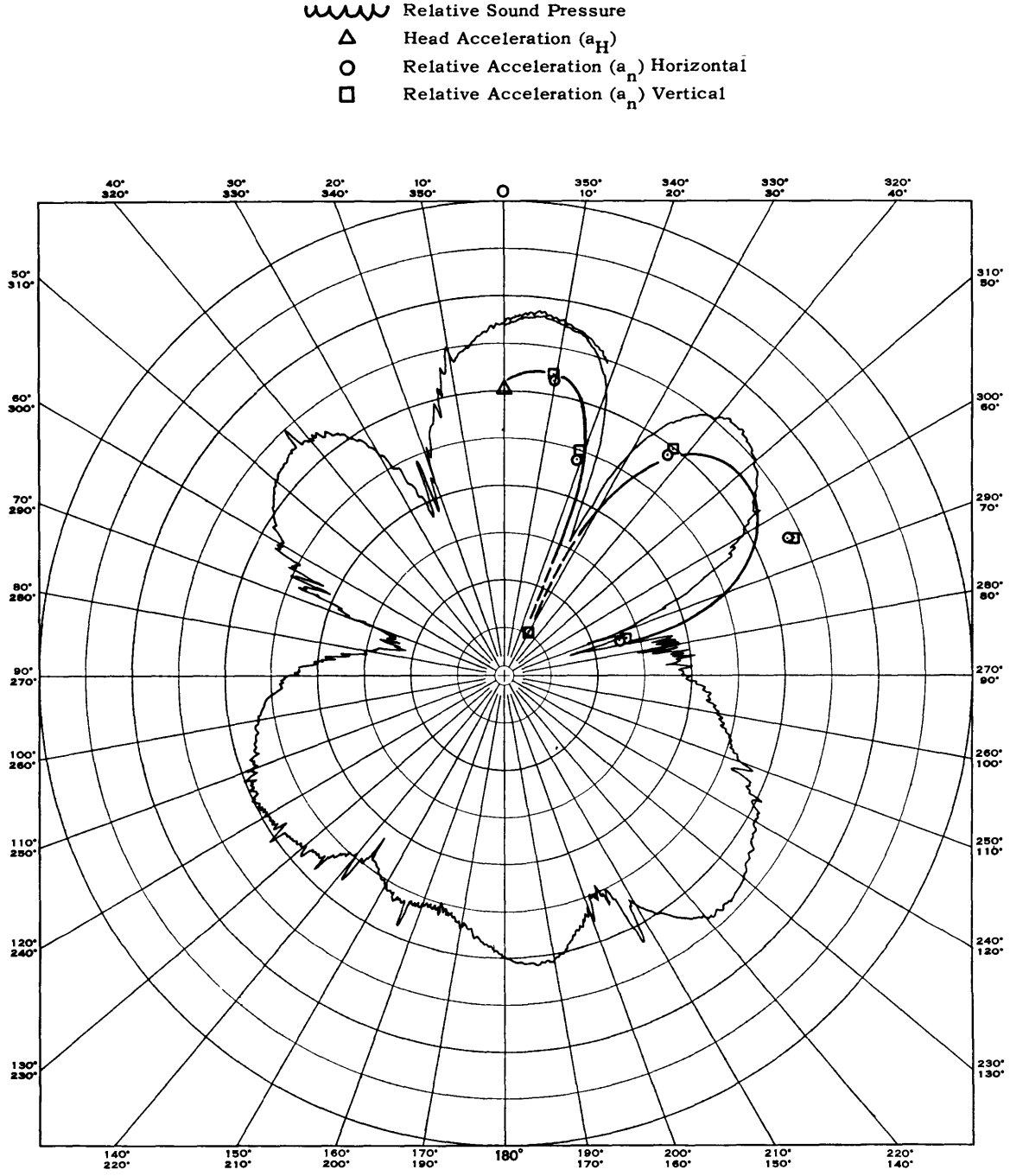

Figure 15h – Model Horizontal (n = 3, m = 3) 3220 CPS

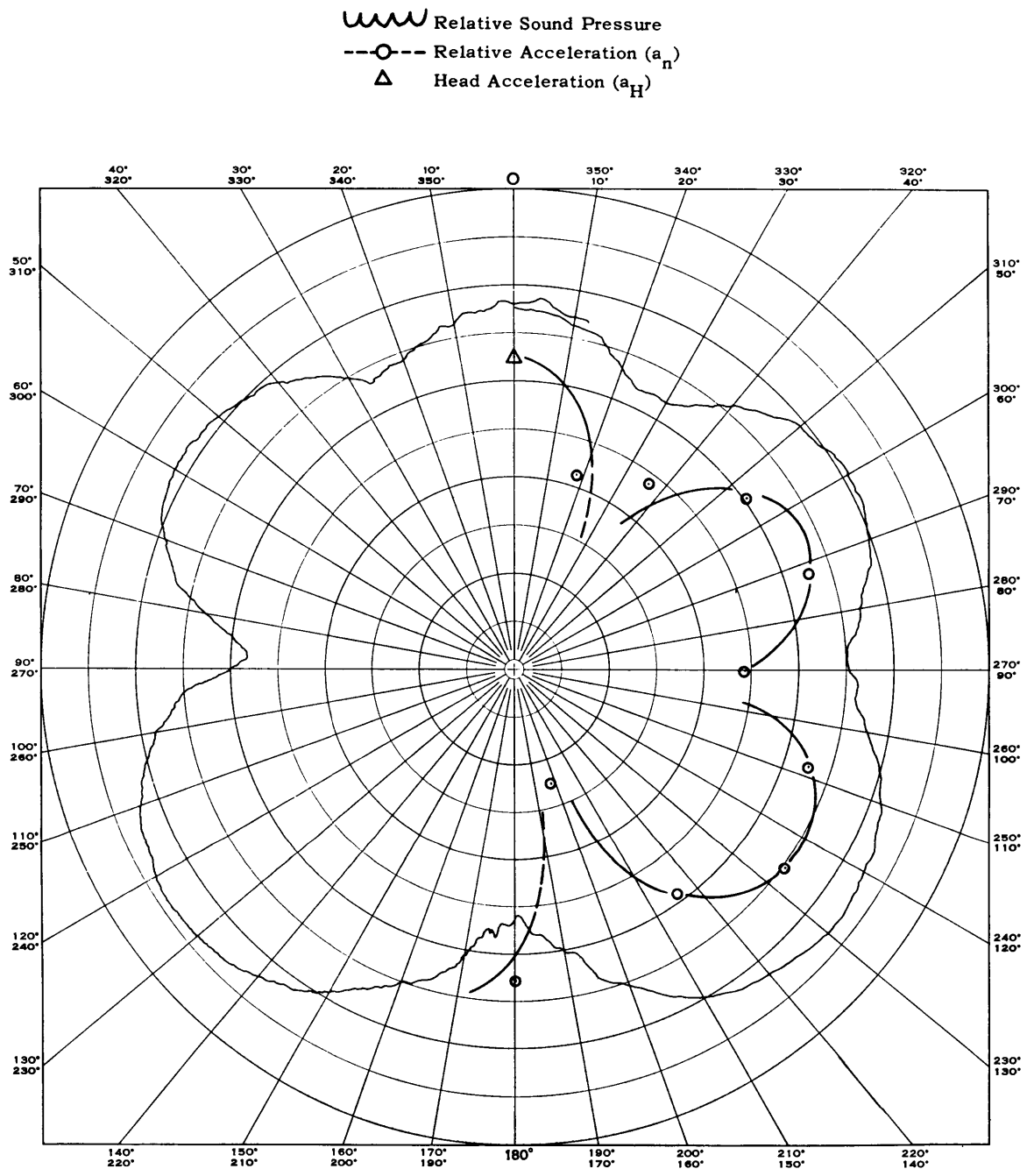

Figure 15i — Model Vertical (n = 3, m = 5) 3670 CPS

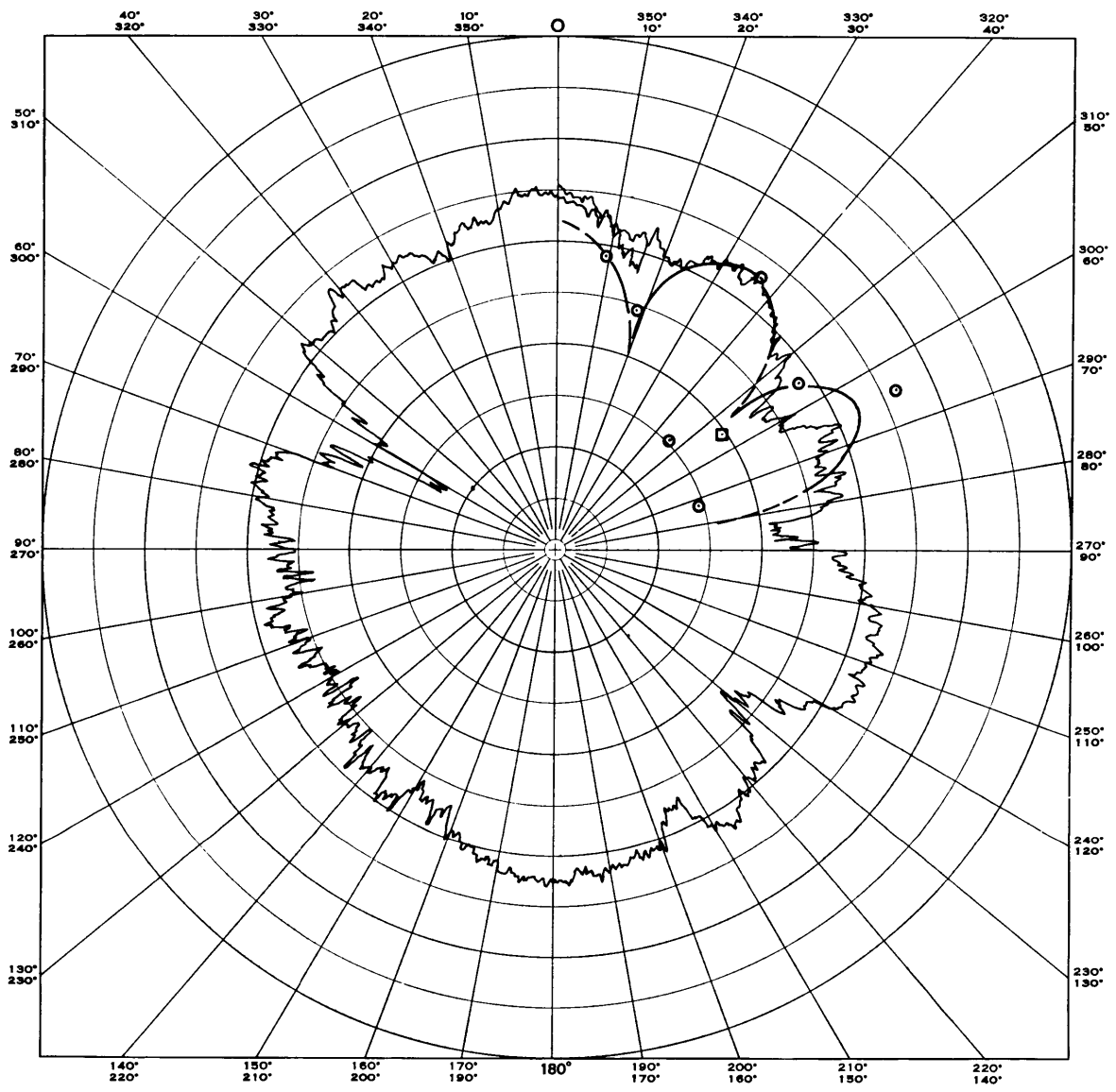

Figure 15j – Model Horizontal (n = 3, m = 5) 3680 CPS

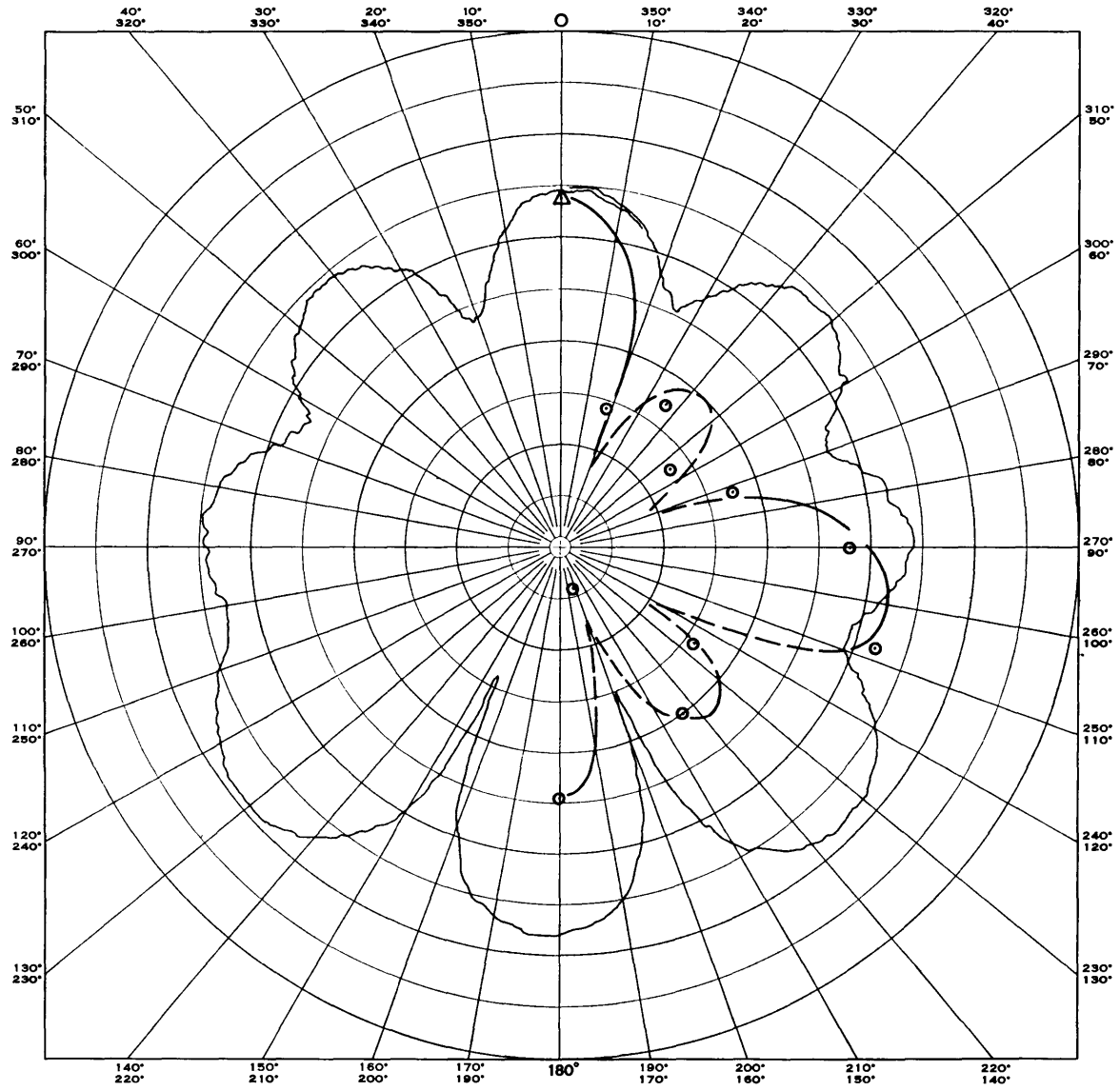

Figure 15k – Model Vertical (n = 4, m = 1) 5270 CPS

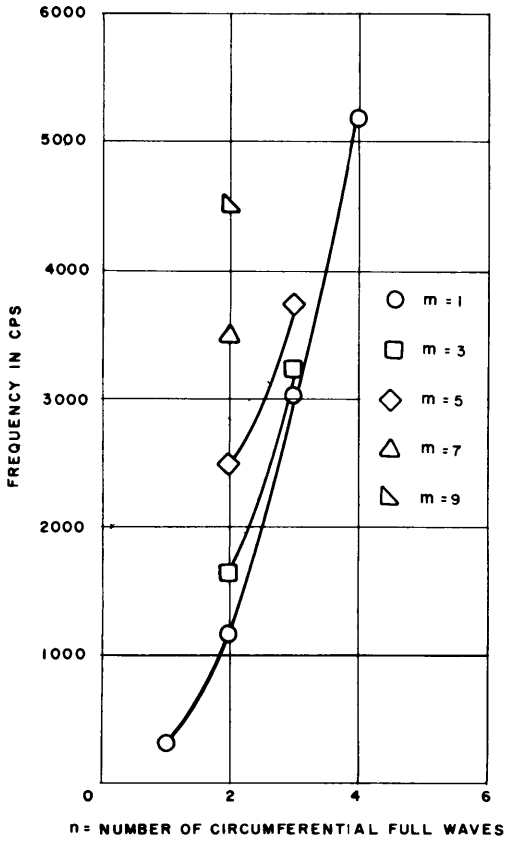

Figure 16a — Number of Circumferential Full Waves (n) versus Frequency

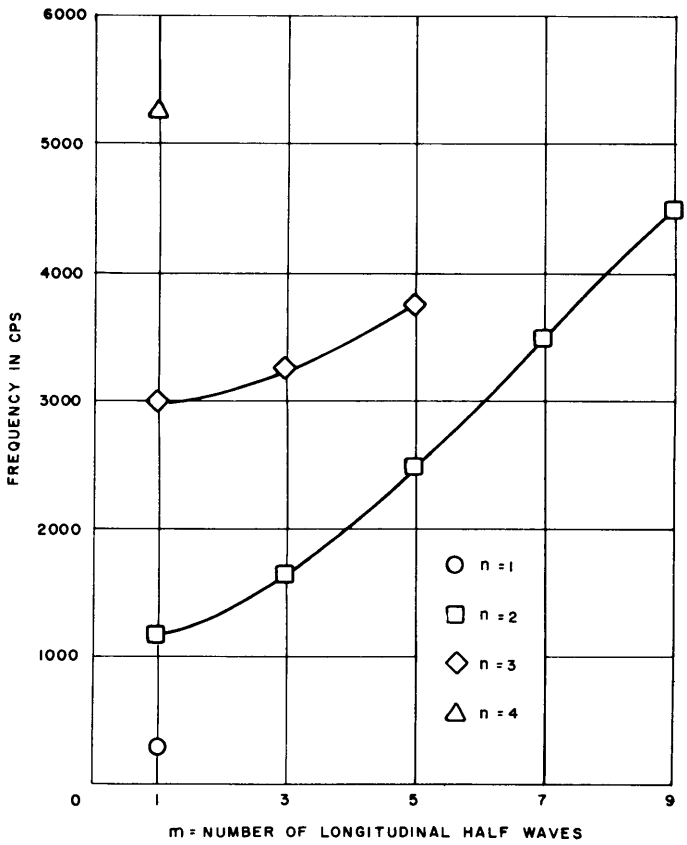

Figure 16b — Number of Longitudinal Half Waves (m) versus Frequency

Figure 16 — Plot of Recognizable Vibration Modes

ACKNOWLEDGMENTS

In accomplishing the objectives of this model study the authors wish to acknowledge the technical assistance rendered by the Naval Ordnance Laboratory Acoustical Facility at Brighton, Maryland, and the following Model Basin personnel: Dr. E. Buchman and Dr. H. Alma for their valuable contributions in the evaluation of the data and compilation of the report; the technical assistance required during instrumentation development from Messrs. R. Tuckerman and F. Schloss; and the careful preparation of the model and instrumentation by Mr. M. Kegel.

REFERENCES

1. Bureau of Ships letter F013-0503 Serial 634 C3-438 of 9 May 1962.

2. Schloss, F., "Recent Advances in the Measurement of Structural Impedance," David Taylor Model Basin Report 1584 (Jan 1963).

3. Williams, K. G. and Coate, M. M., "U.S. Naval Ordnance Laboratory Acoustic Facility," Naval Ordnance Laboratory Report 1198 (Aug 1958).

4. Wright, D. V., et al., "Vibration Transmission and Impedance of Basic Foundation Structures," Westinghouse Research Laboratories Report 62-917-515-R1 (Oct 1962).

5. Stahle, C. V., "A Phase Separation Technique for the Experimental Determination of Normal Vibration Modes of Flight Vehicles," Shock, Vibration, and Associated Environments, Part IV, Bulletin 29, Office of the Secretary of Defense (Jun 1961).

6. Arnold, R. N. and Warburton, G. B., "Flexural Vibrations of the Walls of Thin Cylindrical Shells Having Freely Supported Ends," Proceedings of the Royal Society (London) Vol. 197 (Dec 1948).

7. Brighman, G. A. and Borg, M. F., "An Approximate Solution to the Acoustic Radiation of a Finite Cylinder," Journal of the Acoustical Society of America, Vol. 32, No. 8 (Aug 1960).

INITIAL DISTRIBUTION

Copies	
25	CHBUSHIPS 9 Polymer, Fiber and Pack Sec (Code 634C) 1 Lab Mgt (Code 320) 3 Tech Lib (Code 210L) 1 Struc Mech, Hull Mat & Fab (Code 341A) 1 Matls. Fuels & Cold Weather (Code 342A) 1 Prelim Des Br (Code 420) 1 Prelim Des Sec (Code 421) 1 Ship Protec (Code 423) 1 Hull Des Br (Code 440) 1 Sci & Res Sec (Code 442) 1 Struc Sec (Code 443) 2 Sub Br (Code 525) 1 Hull Arrgt, Fittings & Preserv (Code 633) 1 Pres Ves Sec (Code 651F)
1	CHBUDOCKS, Attn: C-423
4	CHONR 1 Res Coordinator (Code 104) 1 Matl Sci Div (Code 419) 1 Struc Mech Br (Code 439) 1 Undersea Prog (Code 466)
4	CNO 1 Tech Anal and Adv Gr (OP 07T) 1 Plans, Prog & Reg Br (OP 311) 1 Sub Program Br (OP 713) 1 Tech Support Br (OP 725)
2	CO U.S. Naval Applied Sci Lab (Code 9350)
3	CHBUWEPS 1 (Code RRMA) 1 (Code RMMP-23) 1 Special Projects Office S6-27012 (Mr. H. Bernstein)
2	CDR, USNOL 1 W Dept 1 WM Div

Copies	
3	DIR, USNRL 1 (Code 2027) 1 (Code 6120) 1 (Code 6210)
2	DIR, Plastics Tech Evaluation Center, Picatinny Arsenal, Dover
1	CDR, USNOTS (Code 5557), China Lake
1	US Naval Ordnance Test Station (Mr. J. L. Phillips P-8082) Pasadena, California
20	CDR, DDC
1	CO & DIR, USMEL
1	CO & DIR, USNUSL
1	CO & DIR, USNEL
1	CO USNROTC & NAVADMIN U, MIT
1	CO, USNUOS
1	CIR of Def R & E, Attn: Tech Lib
2	NAVSHIPYD PTSMH
1	O-in-C, PGSCOL, Webb Inst
1	Dir, APL, Univ of Wash, Seattle
1	NAS, Attn: Comm on Undersea Warfare
1	CO & DIR, USMDL
2	Commanding General Aeronautical Systems Div (ASRCNC-1) Wright Patterson Air Force Base, Ohio
1	Aerojet-General Corp, (Mr. S. Stokes) Azusa, California
1	NARMCO Research & Dev Div of Telecomputing Corp., San Diego, Calif (Mr. B. Duft)

Copies	
1	Armour Research Foundation (Dr. J. W. Dally) Illinois Inst of Tech Chicago, Ill
1	(Gen Motors Corp.) (Dr. R. B. Costello) Def Systems Div, Santa Barbara Lab Santa Barbara, Calif.
1	Battelle Memorial Inst (Dr. R. Leininger) Columbus, Ohio
1	H. I. Thompson Fiberglass (Mr. N. Meyers) Gardena, Calif.
1	Owens-Corning Fiberglass Corp. (Mr. R. J. Weaver) Washington, D. C.
1	U. S. Rubber Research Center (Mr. E. Francois, Jr.) Wayne, N. J.
1	Shell Chemical Co. (Mr. R. E. Bayes), Plastics & Resin Div, New York, N. Y.
1	North American Aviation Inc. (Mr. R. Gorcey) Rocketdyne Div Canoga Park, Calif.
1	Hercules Powder Co (Mr. J. A. Scherer) Wilmington, Del.
1	Brunswick Corp. (Mr. W. McKay) Marion, Va.
1	Douglas Aircraft Corp. (Mr. J. H. Cunningham) Missile & Space Systems Div. Santa Monica, Calif.
1	Goodyear Aircraft Corp. 1210 Massillon Rd Akron, Ohio
1	A. O. Smith Corporation (Mr. W. A. Deringer) Milwaukee, Wisconsin

Copies	
1	University of Ill. (Prof H. R. Corten) Dept of T & M Urbana, Ill
1	AVCO Corp. Undersea Projects Directorate Wilmington, Mass
1	Union Carbide Plastics Corp. (Mr. Charles Platt) Brunswick, N. J.

David Taylor Model Basin. Report 1867.
MOBILITY AND SOUND RADIATION MEASUREMENTS ON A CYLINDRICAL GLASS-REINFORCED-PLASTIC MODEL, by Dwight L. Ludwig and Christopher J. Noonan. Nov 1964. iii, 38p. illus., diagrs., graphs, refs. UNCLASSIFIED

Vibration and sound radiation characteristics are determined for a 6-in. ID, 28-in. long, internally ring-stiffened, glass-reinforced-plastic cylinder in the frequency range of 200 to 5300 cps. Drive-point mobility, an estimate of damping ratio, the mode shapes of resonant frequencies, the radiated sound pressure levels versus frequency, and the sound pressure directivity patterns at resonances are presented.

1. Cylindrical shells (Stiffened)--Reinforced plastics--Vibration
2. Cylindrical shells (Stiffened)--Reinforced plastics--Acoustic factors
3. Cylindrical shells (Stiffened)--Vibration--Model tests
4. Cylindrical shells (Stiffened)--Acoustic factors--Model tests